Macromolecular Bioscience
www.mbs-journal.de

Designing Polymeric Mixed Conductors and Their Application to Electrochemical-Transistor-Based Biosensors

*Ji Hwan Kim, Seong-Min Kim, Gunwoo Kim, and Myung-Han Yoon**

Organic electrochemical transistors that employ polymeric mixed conductors as their active channels are one of the most prominent biosensor platforms because of their signal amplification capability, low fabrication cost, mechanical flexibility, and various properties tunable through molecular design. For application to biomedical devices, polymeric mixed conductors should fulfill several requirements, such as excellent conductivities of both holes/electrons and ions, long-term operation stability, and decent biocompatibility. However, trade-offs may exist, for instance, one between ionic conduction and overall device stability. In this report, the fundamental understanding of polymeric mixed conductors, the recent advance in enhancing their ionic and electrical conductivity, and their practical applications as biosensors based on organic electrochemical transistors are reviewed. Finally, key strategies are suggested for developing novel polymeric mixed conductors that may exceed the trade-off between device performance and stability.

1. Introduction

The ion permeability in polymeric mixed conductors offers unique advantages as a channel material in active electronic devices such as organic electrochemical transistors (OECTs). The effective modulation of the channel current using gate bias and the activity-dependent responses in neuromorphic/synaptic devices are facilitated by ion permeability into the polymeric network.[1–6] Additionally, the capabilities of redox chemistry-mediated biomolecular sensing,[7–14] ion pumping characteristics,[15,16] in vivo device operation,[17–21] and large volumetric capacitance proved the potential of OECT as a promising biomedical device platform.[1,22]

As an OECT channel, mixed conductors should exhibit efficient transport of ions and electrons/holes as well as the transduction of ionic current into electronic current. These properties are determined by the polymer chain length,[23–25] crystallinity,[26–29] and molecular alignment.[25,30,31] In the case of biomedical use, the prerequisite of mixed conductors is extended to biocompatibility and long-term stability in vivo. Recently, remarkable advances have been made in materials research, and considerable efforts have been invested to satisfy these demands.[32–35] Despite a good number of review articles on organic bioelectronics and OECTs, only a few reviews have focused on the correlation between the molecular structures of mixed conductors and the performance/stability of resultant OECTs as biosensors. In this article, we review the relationship among intramolecular/intermolecular structures, properties, and stability, and provide the suggested ideal structures for high-performance stable OECT-based biosensors. The first part covers mixed conduction by comparing OECTs and electrolyte-gated transistors. Subsequently, we discuss the structure of the most well-known mixed conductor, poly(3,4-ethylenedioxythiophene) doped with poly(styrene sulfonate) (PEDOT:PSS) and the chemical aspects of other ion-permeable conjugated polymers. Next, we address the recent biomedical applications of OECTs to determine the prerequisites for their high device performance and stability in terms of biochemical sensing and bioelectric signal recording in vivo. The last part depicts the structural design criteria investigated in recent publications and, finally, the suggested perspective on the promising chemical structures and the outlook are provided.

2. Organic Electrochemical Transistors

Generally, an OECT employs an electrolyte solution/gel for channel current modulation using gate biases. Seemingly, it operates similar to an electrolyte-gated organic field-effect transistor (EGOFET). However, the actual working principle is different; therefore, understanding their differences provides a clear concept of OECTs. In this section, the differences between these two devices are addressed, and the relevant material characteristics that can aid OECT operation are suggested. Finally, the advantages of OECT over EGOFET are discussed in light of the aforementioned features.

In EGOFET, a bias applied to the polarizable gate electrode induces the migration of ions in the electrolyte, and the ions form an electrical double layer at both the gate–electrolyte and electrolyte–channel interfaces (**Scheme 1**, left) because the active layer is ion-impermeable.[36–39] Due to the electrical

J. H. Kim, G. Kim, Prof. M.-H. Yoon
School of Materials Science and Engineering
Gwangju Institute of Science and Technology
123 Cheomdangwagi-ro, Buk-gu, Gwangju 61005, Republic of Korea
E-mail: mhyoon@gist.ac.kr
Dr. S.-M. Kim
School of Materials Science and Engineering
Georgia Institute of Technology
771 Ferst Dr. NW, Atlanta, GA 30332, USA
The ORCID identification number(s) for the author(s) of this article can be found under https://doi.org/10.1002/mabi.202000211.

DOI: 10.1002/mabi.202000211

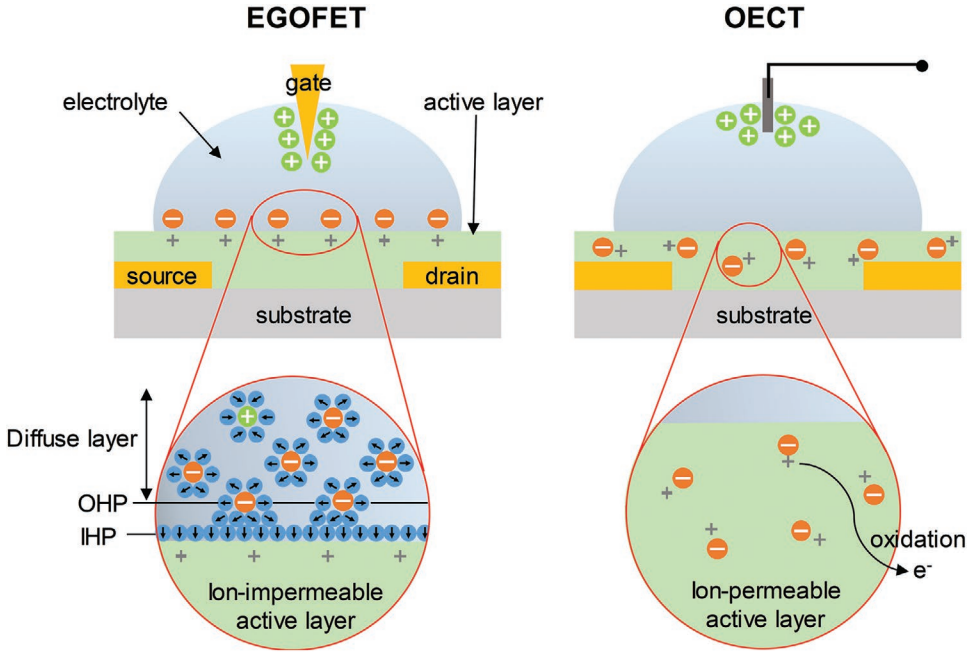

Scheme 1. Device configuration and ion behavior in electrolyte-gated organic field-effect transistors and organic electrochemical transistor.

double layer, the capacitance (1–40 μF cm^{-2}) is higher than that in usual dielectrics, which reduces the operation voltage to a value lower than 2 V, as demonstrated by the previous reports.[40–44] If the active layer is a p-type material, holes accumulate at the electrolyte-active layer interface and the channel conductivity is enhanced significantly when a gate bias is applied. In contrast, the polymeric materials used for OECT typically contain hydrophilic moieties such as ionic functionality or glycol side chains;[3,45–51] the swelling of the active layer in the OECT increases, and ions easily penetrate into the OECT channel. When a bias is applied to the gate, ions in the electrolyte migrate and infiltrate the active layer and charge polymeric chains individually (Scheme 1, right). This process modulates the channel conductance of the OECT more effectively because the entire volume of the channel can act as a capacitive interface; the capacitance can be volumetrically defined and is much higher than that of the EGOFET based on the areal capacitance.[1,2,22] This also contributes to high transconductance values in OECTs. In a typical EGOFET, the areal capacitance of electrical double layer is 1–10 μF cm^{-2},[52,53] while in an OECT with an ≈130 nm thick PEDOT:PSS channel, the (equivalent) areal capacitance is 500 μF cm^{-2}.[22] We suppose that better transconductance of OECT than other transistors could be attributed to this characteristic. However, to charge the 3D capacitor, a large current-carrying ability is required for gate electrodes such as that exhibited by redox gate electrodes or electrodes with large surface areas,[54] and the slow mobility of ions in the active layer (≈10^{-3} cm^2 V^{-1} s^{-1}) limits the time constant to a value of ≈1 ms.[26,55] Moreover, the operation based on electrolytes maintains the channel swelling in water and the transient movement of ions in the electrolyte. These may be related to stability issues.[28] Many studies have suggested the improvement of OECT response time by changing the ion concentration of electrolyte,[56,57] channel dimensions,[22,58] or modifying device configurations,[59–61] but these methods usually involve the trade-off between device performance and stability.

3. Designing Mixed Electronic–Ionic Conductors

3.1. Chemical Aspects of PEDOT:PSS

Although various polymeric materials have been developed and used widely, a comprehensive standard for designing polymeric mixed conductors has not yet been established. After reviewing the electron/hole and ion conduction of PEDOT:PSS, which is one of the most conductive mixed conductors, a generic design standard is suggested in this section.

PEDOT:PSS is the most popular mixed electronic–ionic conductor for OECT studies because it is highly conductive (>1000 S cm^{-1}),[62–69] commercially available, and easy for solution processing. PEDOT:PSS is typically synthesized in the aqueous phase through the oxidative polymerization of ethylenedioxythiophene in the presence of PSS, and the resultant PEDOT:PSS particles in water are composed of a PEDOT-rich core and PSS-rich shells (**Scheme 2**a).[70–74] These two moieties have different charge-transport characteristics due to their dominant components. PEDOT is a π-conjugated polymer which conducts holes through the backbone with overlapped p-orbitals (Scheme 2b, left), whereas PSS is a type of polyelectrolyte with sulfonate as the electrolyte repeating unit, which conducts ions (Scheme 2b, right). Accordingly, the electrical conductivity of PEDOT:PSS is closely related to the structural and chemical properties of the PEDOT-dominant region, and its ion-relevant characteristics are mainly affected by the PSS-rich region.

The electrical/ionic conductivity of a conjugated polymer is governed by the corresponding charge carrier concentration and mobility.[75,76] The electrical conductivity of PEDOT:PSS can be

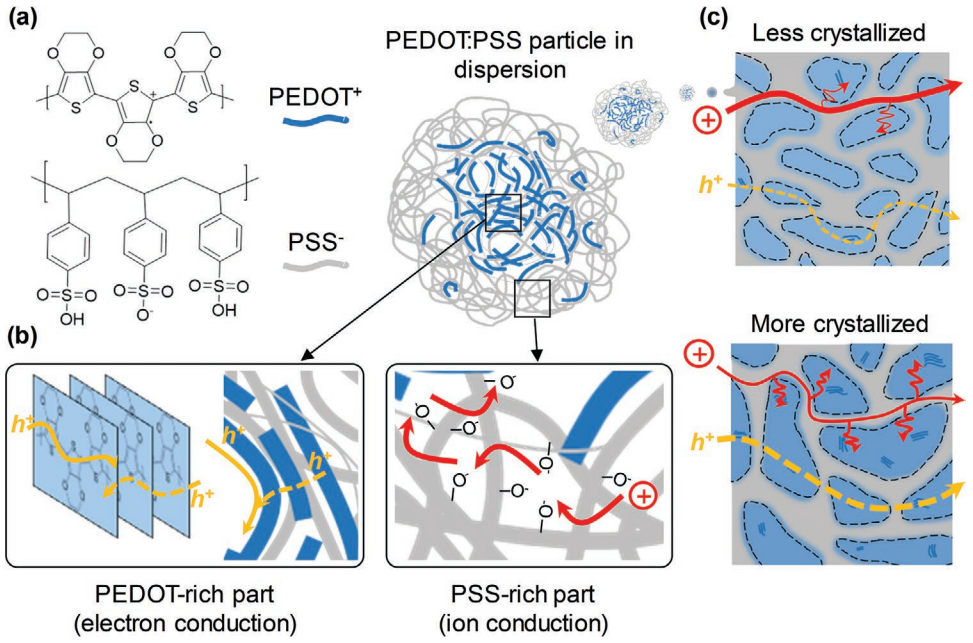

Scheme 2. a) Chemical structure of PEDOT:PSS and a schematic image of the PEDOT:PSS particle microstructure. b) Schematic images of the PEDOT-rich core region and PSS-rich region in the PEDOT:PSS particle. c) Schematic representation of the PEDOT:PSS film microstructure with c) low (upper) and high (low) crystallinity. Adopted under the terms of the Creative Commons Attribution 4.0 International License.[26] Copyright 2016, The Authors, published by Springer Nature.

increased by rearranging the polymer microstructure and/or by removing the electronically insulating portion. Enhancing the crystallinity in PEDOT by changing its conformation from a tangled structure to a linear one facilitates the interchain interaction and increases the charge carrier mobility.[65,69,77–79] Additionally, the post-treatment of PEDOT:PSS film with a strong acid (e.g., sulfuric acid) leads to the removal of excess PSS that is not involved in the doping of PEDOT, increasing the number of conductive moieties in the consequent PEDOT:PSS film.[80–83] To enhance ion conductivity, a high ion concentration should be achieved by employing highly dissociative salt that does not exhibit ion-pair formation or include other species that impede ion motion. In other words, the solvation energy of the ions within the polymer must be more negative than the lattice energy of the salt. Ion mobility is directly related to the movement of ions, which is achieved by ion hopping from a current solvation site to a nearby open site;[84–86] hence, the probability of hopping is increased by the local fluctuation of polymer chains.[87,88] This means that loosely bound polymer chains with low crystallinity are considered to have the enhanced ion mobility. Indeed, one of the recent studies on conducting polymers reported that the ion mobility in a mixed conductor is inversely proportional to its crystallinity (Scheme 2c). Therefore, the electrical conductivity can be improved by increasing the proportion of highly crystallized conductive regions; the ion conductivity can be enhanced by introducing functional groups containing proper counterions in combination with high dissociation characteristics. From this perspective, one of the most successful channel materials using electrolyte salts or polyelectrolytes is PEDOT:PSS in terms of electrical conductivity, processability, mechanical properties, and chemical and environmental stability.[89–92] The details are mentioned in Section 3.1. OECTs employing PEDOT:PSS as the channel exhibit a transconductance of ≈1.2 mS, on and off time constants of 0.5 and 0.02 s, respectively (for a channel w of 200 µm), and on–off current ratios exceeding 10^5. Additionally, the devices can be fabricated on flexible substrates using screen-printing methods and operated under ambient and aqueous electrolyte conditions.[93–96] The optimization of the device response time has also been conducted consistently, and a time constant of ≈100 µs was achieved in one of the recent reports (for a channel w of 15 µm, l of 6 µm, and d of 80 nm).[53] However, one of the critical limitations of PEDOT:PSS is the acidity of PSS, causing the corrosion of materials near the active channel.[97–100] The effect of doping PEDOT with polyelectrolytes which are less acidic than PSS (e.g., (trifluoromethylsulfonyl) imide (TFSI)) was investigated while the distance between the polymer backbone and TFSI, molecular weight of polyanions, and different counterions were varied.[46] The polyelectrolyte polymerized using methacrylate exhibited the poorest device performance (transconductance of 1.65 mS, response time of 178 µs, and conductivity of 8 S cm^{-1}), and the molecular weight and counterion effects were negligible. Nonetheless, it was observed that there exists a correlation among swelling behavior, transconductance, and ion conductivity.

3.2. Other Water-Permeable Conjugated Polymers

Considering that a conjugated polymer with ion permeability is a prerequisite for OECT channels, some water-permeable conjugate polymers contain hydrophilic moieties such as glycol or side chains with counterions as a common feature in their structures. The structural and chemical differences among polymers with diverse functional groups can affect the electrical

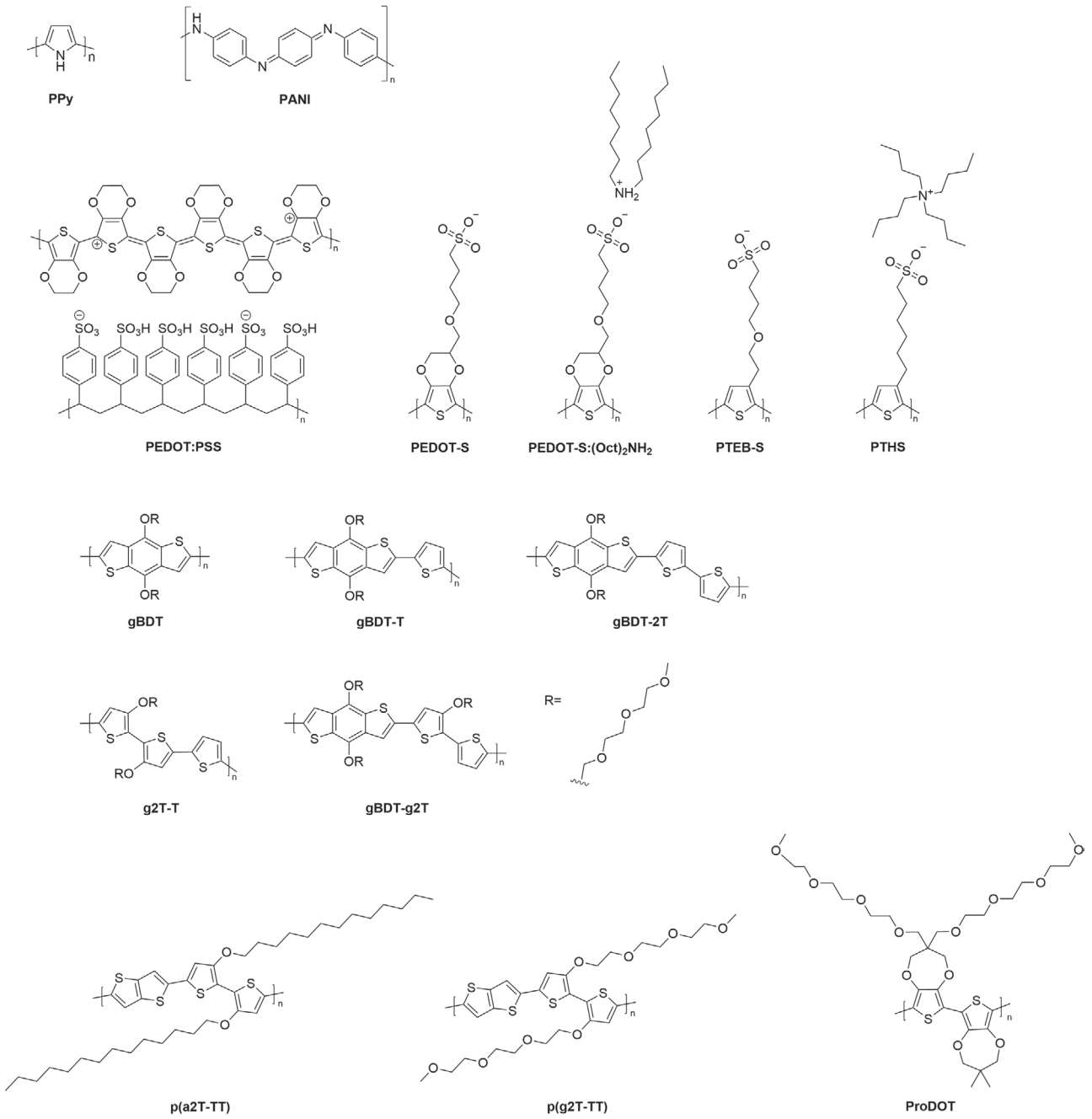

Figure 1. Chemical structures of the various p-type conjugated polymers used for OECT channel materials.

and mechanical properties of mixed conductors and the operation mechanism in the corresponding OECTs. Therefore, in this section, representative mixed conductors with different functional groups are discussed.

3.2.1. p-Type Materials

Figure 1 shows representative p-type mixed conductive polymers. Polypyrrole (PPy) is the first material employed as the channel in OECT, but the device response was relatively slow (≈10 s for a channel width, *w,* and length, *l,* of 1.4 µm) and not durable because spontaneous crosslinking occurs in doped polymers.[101] Additionally, its vulnerability to irreversible oxidation renders devices inoperable; therefore, PPy has seldom been considered for more sophisticated applications. Polyaniline (PANI) can be reduced and oxidized reversibly in air or aqueous electrolyte conditions, and the corresponding OECT exhibits decent device performance and stability, as exemplified by its response time (≈50 ms for a channel *w* and *l* of 1.7 µm and depth *d* of 5 µm), transconductance (0.4 mS at +0.15 V), and drain current retention of up to 80% after 10 h, which

exceed those of the PPy-based OECT.[102] In this study, a PANI-based OECT was used for pH sensing by employing the redox state change of PANI from a highly conductive emeraldine salt to a poorly conducting emeraldine base form. However, the emeraldine state, which exhibits the highest conductivity among redox states, including leucoemeraldine and pernigraniline, can be obtained under acidic conditions (<pH 5) or in the presence of high-molecular-weight polyelectrolytes such as poly(vinyl sulfonate) and poly(styrene sulfonate).[103] Additionally, the low processability, brittleness, and inflammability of PPy are limiting factors for bioelectronics.

In parallel, the electrochemical charging of the active channel has been examined using polymer semiconductors such as poly(3-hexylthiophene) (P3HT),[36,40,43,44] poly (3,3‴-di-didodecylquaterthiophene (PQT-12),[36] poly(9,9-dioctylfluorene-alt-bithiophene) (F8T2),[36] and poly[2,5-bis(3-tetradecylthiophen-2-yl)thieno[3,2-b]thiophene] (PBTTT-C14) in combination with various types of electrolyte salts or polyelectrolytes,[104,105] such as trifluoromethanesulfonic acid, lithium perchlorate, lithium bis(trifluoromethanesulfonyl)imide, and polyethylene oxide. Note that the abovementioned channel materials and electrolytes satisfy the condition of ion permeation into the OECT channel.

Recently, with the emerging biosensor application, the accumulation-mode OECT has become an interesting topic because it is off at the zero gate bias, leading to low power consumption. Considering that the majority of known ion-impermeable polymer semiconductors cannot be applied to accumulation-mode OECTs, conjugated polymer electrolytes are good candidates for accumulation-mode OECTs. One strategy involves attaching hydrophilic ionic side chains that can absorb water molecules to the conjugated polymer; hence, the ion permeability is significantly increased as shown in poly(6-(thiophene-3-yl)hexane-1-sulfonate) tetrabutylammonium (PTHS).[3] The corresponding OECT performance parameters were an improvement over and/or comparable to those of PEDOT:PSS after mixing with ethylene glycol; the transconductance was 0.4 mS at V_G = –0.4 V, the on–off current ratio was ≈700, and the response time was 38 ms. Another example is PSS-free self-doped PEDOT, i.e., poly(4-(2,3-dihydrothieno-(3,4-*b*)-(1,4)dioxin-2-yl-methoxy)-1-butanesulfonic acid, sodium salt) (PEDOT-S). The resultant polymer film was highly conductive and uniform, but external counterions were not required to balance the doped charges in the conjugated polymer backbone. Furthermore, the solubility in polar solvents increased significantly.[106,107] The attempt to use PEDOT-S as an OECT channel was conducted by blending it with poly(2-(3-thienyl) ethoxy-4-butylsulfonate) (PTEB-S), which is a negatively charged polyelectrolyte.[45] In the PEDOT-S OECT, the transconductance was 15.1 mS at V_G = 0.2 V, the on–off ratio was ≈650, and the on and off response times were 360 and 300 ms, respectively. Note that the PTEB-S only OECT exhibited relatively poor performance as represented by a transconductance of 0.7 mS, on–off current ratio of 310, and on and off time constants of 6900 and 400 ms, respectively. The OECT using a polymer blend with a mixing ratio of 3:2 (PTEB-S:PEDOT-S) exhibited a transconductance of 8.5 mS and an on–off current ratio of 530, which were comparable to those of PEDOT-S, but the on and off response times significantly decreased to 192 and 40 ms, respectively. The authors attributed the apparent enhancement in ion transport to the rougher fibrillar morphology, which may facilitate ion percolation.[3] Other studies examined the effect of counterions in polymer blends based on metallic PEDOT-S and semiconducting PTHS, leading to the conclusion that the threshold voltage was shifted by the counterion exchange,[48] and the steric hindrance of counterions affects the stability of PEDOT-S OECTs.[47] Consequently, OECTs based on conjugated polymer electrolytes have the potential for use as various sensors and bioelectronics.

The most recent advance in the development of ion-permeable polymers involve glycolated semiconducting polymers (GSPs), where conjugated polymer semiconductors are derivatized with glycol side chains. In this approach, the transistor operation mode is mainly attributed to bulk doping without ionic functional groups.[49] One of the most promising GSPs is poly(2-(3,3′-bis(2-(2-(2-methoxyethoxy)ethoxy)ethoxy)-[2,2′-bithiophen]-5)yl) thieno[3,2-b] thiophene), p(g2T-TT), in which triethylene glycol is tethered to a polymer backbone composed of bithiophene-thienothiophene (2T-TT). This polymer exhibited higher swelling and ion-permeation properties than the tetradecyloxy-functionalized polymer, poly(2-(3,3′-bis(tetradecyloxy)-[2,2′-bithiophen]-5-yl)thieno[3,2-b]thiophene, p(a2T-TT) because the ethylene glycol side chain is more favorable for water uptake. Therefore, the capacitance, on-current, on–off current ratio, transconductance, ion mobility, and hole mobility of p(g2T-TT) OECT devices were much higher than those of p(a2T-TT). In another study, molecular structural parameters such as polymer backbone, sidechain orientation, and sidechain density were judiciously controlled to determine how the consequent polymer chain orientation and π–π interaction affect electrochromic properties, hole mobilities, and OECT characteristics.[50] The resultant OECT using g2T-T showed a peak transconductance of 7.9 mS at a gate voltage of –0.6 V, on–off current ratio above 10^5, and response time of 0.64 ms for a channel *w* of 10 μm, *l* of 10 μm, and thickness of 103 nm. Additionally, PEDOT functionalized with glycol side chains was reported to take advantage of the exceptional redox stability of PEDOT-based polymers.[51] In this study, the prepared OECT devices exhibited a transconductance of 0.6 mS at a gate voltage of –0.7 V, on–off current ratio exceeding 10^5, and response time of <1 s measured from an optical contrast change (film area of 2 cm^2 and thickness of 200 nm).

3.2.2. n-Type Materials

Although n-type channel materials are important for complementary circuits that have advantages such as low-power driving and noise minimization, developing them has always been challenging because of their susceptibility to oxidization,[108] and the same behavior of low work function metals such as Al, Mg, or Ca, which have a lower electron injection barrier to n-type materials.[109] Furthermore, n-type materials for OECTs require a few more conditions: the material should be stable in an aqueous electrolyte, reversibly reduced and oxidized within the electrochemical window provided by the electrolyte, ion-permeable, and have a high charge carrier mobility. The first reported n-type OECT material was a polymer composed of a 2,6-dibromonaphthalene-1,4,5,8-tetracarboxylic diimide (NDI) monomer and linear glycol side chains with several ethylene glycol repeating units (**Figure 2**).[110] The diimide and bithiophene units and their hybridized energy levels resulted in high

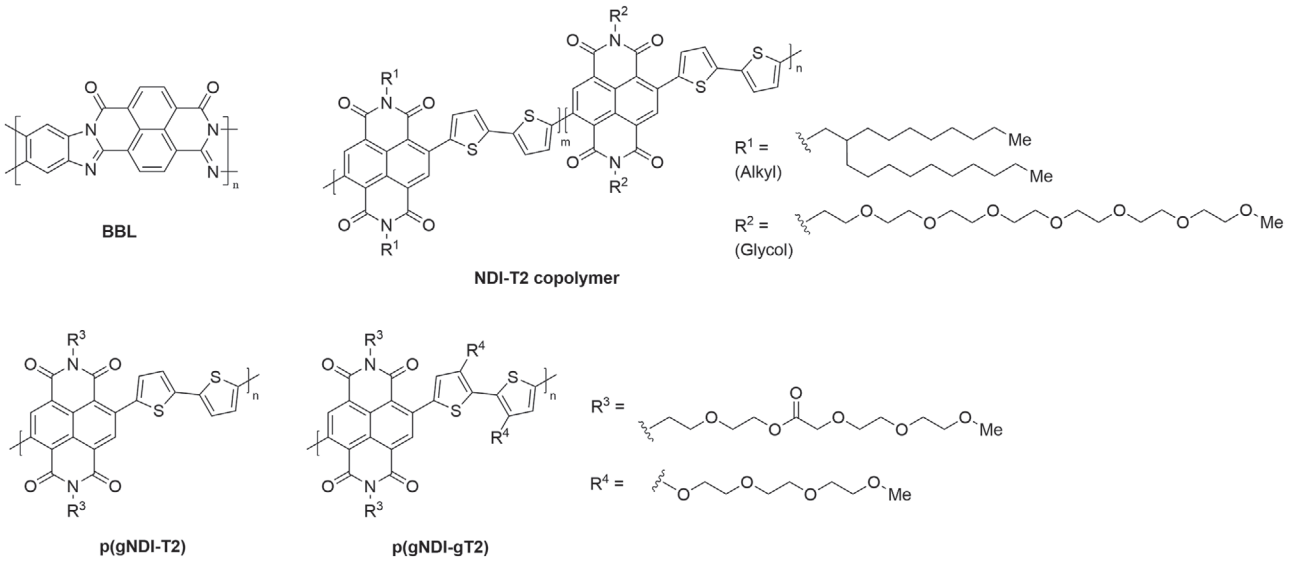

Figure 2. Chemical structures of the various n-type conjugated polymers used for OECT channel materials.

electron affinities and low ionization potentials, making n-type OECT materials look promising. The transconductance of the OECT was 21.7 μS at a gate voltage of 0.5 V with an on–off ratio higher than 10^3, and the device was operated for 2 h without degradation. The authors suggested that the low electron mobility (1.0×10^{-5} cm^{-2} V^{-1} s^{-1}) of p(gNDI-gT2) was the limiting factor for drain currents and transconductances that are higher compared to previous accumulation-mode OECTs.[41,49,50] Another candidate is the ladder-type poly(benzimidazobenzoph enanthroline) (BBL).[111] Because the ladder structure provides rigidity and planarity of the π-conjugated polymer backbone, the delocalization of the carriers in BBL facilitates intramolecular transfer; therefore, the delocalization provides high polaron mobility along the chain,[112] and the integrated redox active sites of BBL ensure high n-dopability, which is essential for an OECT channel.[113] The OECT exhibited a transconductance of 9.7 mS at a gate voltage of 0.6 V, on–off ratio higher than 6×10^3, and on and off response times of 0.9 and 0.2 s, respectively (for a channel w of 39 mm, l of 20 μm, and thickness of 180 nm). Additionally, the OECT exhibited no current degradation during successive gate voltage pulses (V_G = 0.5 V, pulse length = 5 s) for 1 h and after three months of storage in air, and the transconductance and drain current of the device remained unaffected. The high transconductance and stability of the OECT using the BBL were attributed to the high electron transport characteristics resulting from the ladder-type chain and electron affinity of the polymer itself.

4. Applications of Organic Electrochemical Transistors

4.1. Biomolecular Sensors

The detection of biomolecules is one of the most important function expected of biomedical devices. Biomolecule detection is a means of checking the health status of patients, diagnosing diseases early, and determining the effects of drugs by measuring the concentration of various metabolic mediators in vivo. There exist two types of OECT sensors where biomolecular sensing takes places at either active layer or gate electrode: the active layer is treated for enzyme fixation so that the channel conductance can be modulated directly, or the gate electrode is modified in the similar manner so that the channel current can be affected by the modified gate capacitance. Despite the difference in actual sensing location, however, both types of OECT sensors require the same properties such as high transconductance and operational stability. The molecular selectivity of channel materials has been most actively studied in OECTs as biomolecular sensors because most of the biomolecules of interest have only one enzyme-bearing receptor. Additionally, for a stable and repetitive operation of the device, enzyme fixation on the channel is considered essential.[8–10,12,114,115] Many studies have been conducted on the methods of immobilizing an enzyme on a channel, primarily using the entrapment method,[8,13,116–119] or fixing through covalent bonding.[9,10,12] Because the others, such as physical adsorption, did not possess long-term stability.[95,120] In this section, we focused on the processes immobilizing enzymes and operational stability of the biomolecular sensors, as summarized in **Table 1**. Dissolving enzymes in ionic gels with a small amount of water is very easy, and these enzymes have been reported to be stable over 18 months.[13] In addition, various methods have been proposed for covalent bonding, such as mixing active channels with a photo-crosslinkable hydrogel,[8] or the reaction between human epidermal growth receptor 2 (HER2) and HER2 antibodies.[121] The device fabricated for detecting protein biomarkers was prepared as follows: the gate electrode of the OECT was modified using mecaptoacetic acid, and an HER2 antibody was attached to the gate electrode. Subsequently, through a reaction between HER2 and the antibody, HER2 was attached to the electrode, and finally, catalytic nanoprobes were added to the HER2. The nanoprobe was an electrochemically active enzyme, horseradish peroxidase.[122] However, a widely used method is immobilizing

Table 1. Various electronic/ionic mixed conductors employed as active channel in OECT biosensors.

References	Mixed conductors	Analytes	Enzyme fixation method	Main results
Pappa et al. (2018)[7]	P90	Lactate		Direct lactate detection without electron mediator and enzyme fixation
Strakosas et al. (2017)[8]	PEDOT:PSS-PVA	Lactate, glucose	Entrapping into PEG-DA hydrogel	Monitoring of cell metabolism using OECT sensors prepared by fixation of various enzyme into hydrogels
Pappa et al. (2016)[10]	PEDOT:PSS-PVA	Glucose, lactate, cholesterol	Tethering enzyme-fixed chitosan with crosslinker	On-chip multianalyte detection in saliva using the OECT array
Welch et al. (2015)[12]	PEDOT:PSS	Glucose	Immobilizing enzyme on the polymer brush grown on the active layer	Highly stable (≈100 days) responses of OECT-based sensor
Khodagholy et al. (2012)[13]	PEDOT:PSS	Lactate	Embedding enzyme into ionogel which acts as solid electrolyte	Development of highly stable and flexible solid-state sensor
Wustoni et al. (2019)[14]	PEDOT:PSS/PAAm:PBA composite	Glucose	Electropolymerizing EDOT and PSS with pre-gel (PBA and acrylamide)	Development of enzyme-free metabolite sensor
Tang et al. (2011)[114]	PEDOT:PSS	Glucose	Drop-casting chitosan-MWCNT hybrid solution onto GOx drop-cast on Pt electrode	Highly sensitive (detection limit of 5×10^{-3} M) OECT-based glucose sensor by incorporating conductive nano materials
Liao et al. (2015)[95]	PEDOT:PSS	Dopamine, ascorbic acid, uric acid	Drop-casting on GO/PANI/nafion-graphene film	Highly sensitive (detection limit of 3×10^{-9} M) and selective molecular sensors
Bernards et al. (2007)[115]	PEDOT:PSS	Glucose	Using enzyme-enzyme dispersed electrolyte (without fixation)	Demonstration of device operation and elucidating device physics
Bartlett et al. (1998)[117]	Polyaniline	Glucose	Entrapping enzyme in poly(1,2-diaminobenzene) film electrochemically deposited on top of the polyaniline	First demonstration of enzyme-based electrochemical transistor sensor
Yang et al. (2010)[118]	PEDOT:PSS	Glucose	Using ionic liquids as a reservoir for the enzyme and the mediator	Demonstration of ionic liquids as a good candidate for immobilization of enzymes
Liao et al. (2015)[119]	PEDOT:PSS	Glucose	Drop-casting GOx-chitosan mixture solution on gate electrode	Fabrication of compact chip size of OECT-based multianalyte sensing devices

enzymes after fixing relatively short molecules such as silane after plasma treatment,[12] which result in devices that retain 100% of the response over 100 days with a slight increase in the standard deviation from 14% to 25%. Recently, devices capable of sensing without a mediator have been reported using an n-type NDI-based polymer with electron-accepting properties (**Figure 3**a).[7] The glycol side chains of the polymer provide polar groups for the enzyme to interact with;[123] therefore, the fixation procedure of the enzyme is significantly simplified to placing the device into the enzyme-dispersed water. Figure 3b indicates that the device has activity only on the lactate and none on hydrogen peroxide, confirming the direct electron transport from lactate oxidase to the active layer without a mediator. Additionally, the authors suggested a new possibility for the sensitivity modulation of a device by controlling the gate bias by using an n-type accumulation-mode material. Furthermore, the implementation of a fourth-generation glucose sensor capable of directly sensing a target molecule using a conductive hydrogel was reported last year.[14] PEDOT:PSS and a poly(acrylamide) gel functionalized with phenylboronic acid (PAAm:PBA) were prepared using electropolymerization at a single step on gold-coated substrates (Figure 3c). PEDOT:PSS acted as the electronic transducer and the PAAm gel as a scaffold that accommodates the PBA units that are complexed with glucose (Figure 3d). The PBA part binds with glucose and causes the charged site to induce changes in the volume, impedance, and capacitance of the material. These changes originated from the change in glucose concentration only in blood-like conditions, and the output signal of the OECT bearing conductive hydrogel as its gate electrode was many times higher than the current measured using an amperometric electrode (Figure 3e).

4.2. Electroactive Signal Recorders

In addition to diseases associated with metabolism, neurological and heart diseases occur frequently because of the life patterns of modern people. Dementia, epilepsy, angina pectoris, and arrhythmia, which are related to electroactive cells such as neurons or cardiomyocytes, can be prevented and diagnosed by analyzing electroactive signals from the body. Therefore, electroactive signal recorders with high spatial and temporal resolution and high signal-to-noise ratio must be developed for accurate diagnosis and analysis. A multielectrode array (MEA) is a specialized tool for this purpose because it has a high spatial and temporal resolution.[124–126] This effect can be maximized when the OECT is applied to the MEA instead of the needle-type probe developed earlier because the organic channel has lower stiffness to decrease the generation of thrombi and glial cells, which are insulators. This makes measuring electrical activity chronically easier. Recently, OECT arrays combined with MEAs were developed to decrease the rigidity of materials,[15,18]

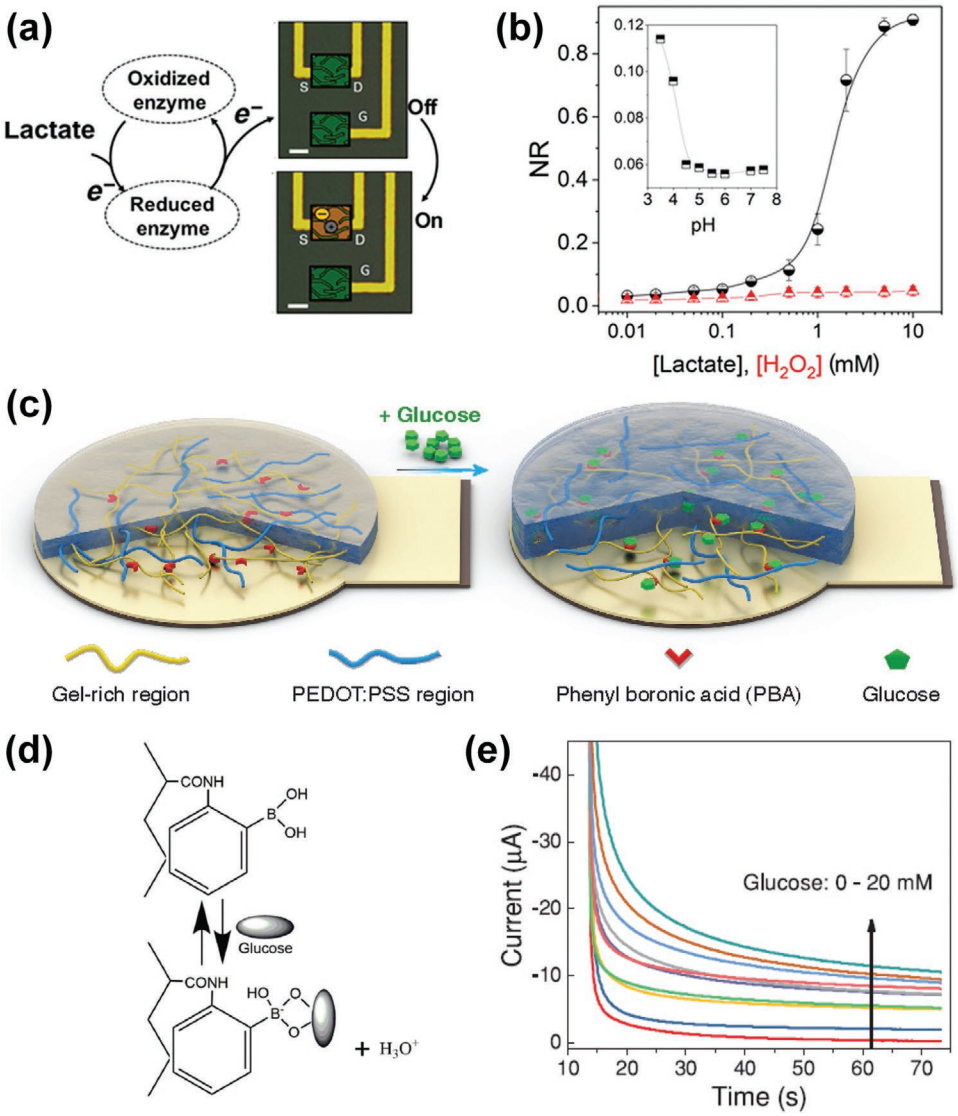

Figure 3. a) Schematic of the OECT biomolecular sensor showing the interactions among the enzyme, LOx, and n-type channel. b) Normalized response of the OECT to H_2O_2 (red triangles) and to the lactate in the presence of LOx (black circles). The inset depicts the sensitivity of the device to pH. Reproduced under the terms of the Creative Commons Attribution 4.0 International License.[7] Copyright 2018, The Authors published by American Association for the Advancement of Science. c) Illustration of the sensing scheme: Swelling of the conductive gel upon binding of glucose changes its electrical response. d) Illustration of the binding event between glucose and the PBA units on the PAAm chain. e) Change in the electrode current upon successive additions of glucose. Reproduced with permission.[14] Copyright 2019, Wiley-VCH.

and to use a material that neither responds to the body's immune system as a substrate nor wraps the rigid part of the device.[17,20,21,56] An OECT covered with parylene, except for the active channel area, can be a representative example. This device was prepared on a relatively rigid SU-8 shuttle; then, the shuttle was moved to the target point and used to transfer the device into the body. The embedded device exhibited stable operation for a month without glial response.[21] Another candidate is poly(3-methoxypropyl acrylate) (PMC3A), which has ion conductivity and antithrombotic properties (**Figure 4**a).[17] This unique material is used to wrap the entire device to prevent the formation of thrombi and transport external ions into the channel of OECTs. Hence, the device exhibits superior performance (transconductance of 1 mS, signal-to-noise ratio of 52 dB, and response time of 60 μs) and stable operation even in the platelet suspensions (the response time change was negligible after 2 h). In addition, highly stretchable characteristics induced by the grid structure of the device caused it to adhere to the tissue of interest; hence, a significantly high signal-to-noise ratio was obtained (Figure 4b,c).[17,18] Another approach was conducted to increase the power efficiency of an electroactive signal recorder, which is the subthreshold operation of OECTs.[127] As reported for metal-oxide-semiconductor field-effect transistor-based biosensors, the subthreshold region of a transistor has a significantly higher power efficiency than the superthreshold region because the transconductance efficiency is significantly higher in this region (Figure 4d).[128,129] The authors concluded that this phenomenon was valid for OECTs, and the operational

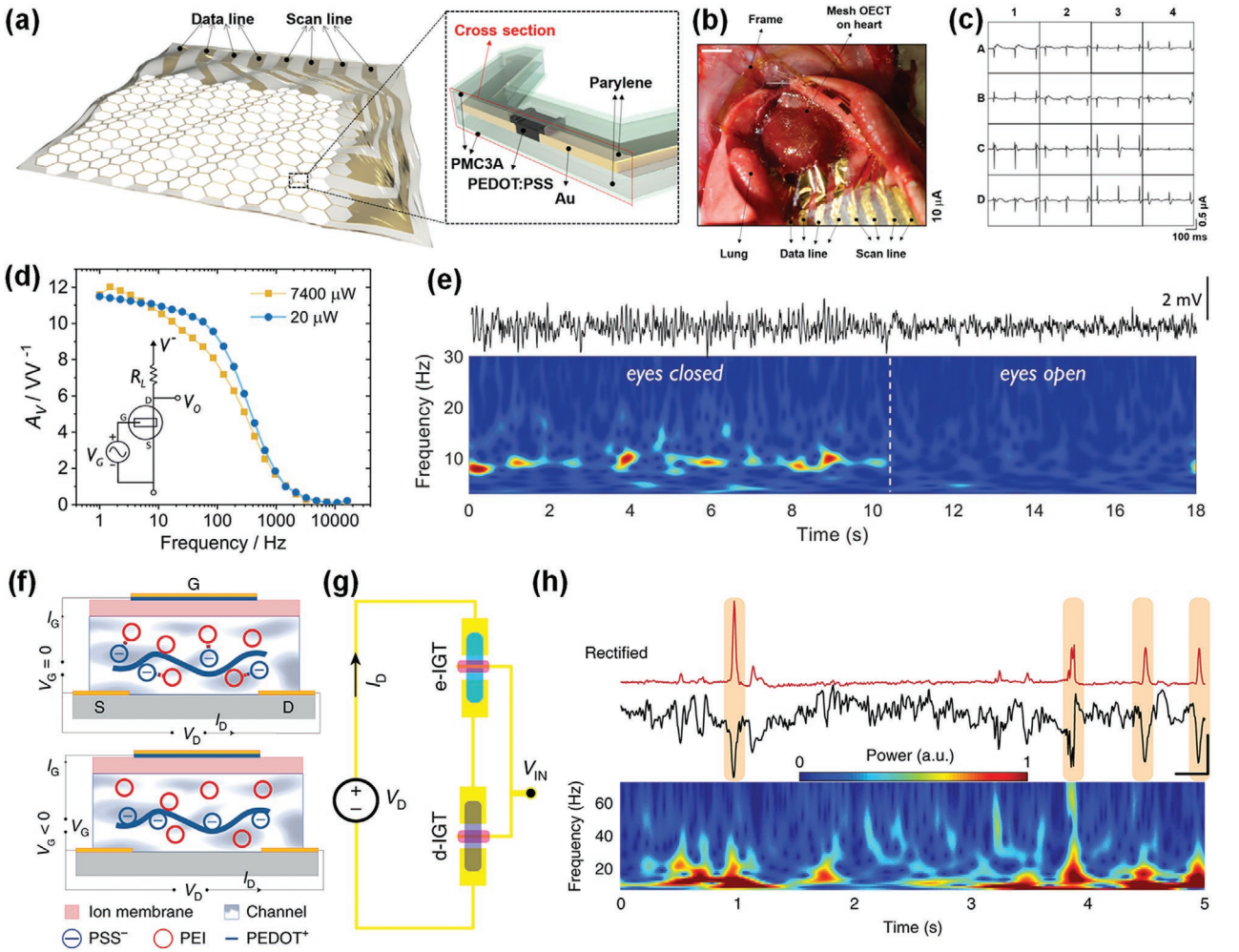

Figure 4. a) Image of the stretchable electrophysiology OECT array on a honeycomb grid parylene substrate and cross section of the stretchable OECT array. b) Image of the positioning of the 4 × 4 OECT array on the heart of a rat. c) ECG signals from a multiplexed 4 × 4 OECT array. Reproduced under the terms of the Creative Commons Attribution 4.0 International License.[17] Copyright 2018, The Authors published by American Association for the Advancement of Science. d) Performance comparison of subthreshold (blue circles) and superthreshold (orange squares) regimes. The voltage gain bandwidth indicates similar results for both regions; however, the subthreshold operation consumes ≈370 × less power. e) EEG voltage output signal measured in the subthreshold region showing alpha rhythm response (top), and the corresponding time–frequency plot (bottom) showing changes in signal content depending on the eyes being closed and opened. Reproduced under the terms of the Creative Commons Attribution 4.0 International License.[127] Copyright 2018, The Authors, published by Wiley-VCH. f) Schematic diagram of enhancement-mode ion-gated transistor cross-section and wiring diagram for device operation. g) Schematic of a nonlinear signal rectification circuit composed of a depletion-mode ion-gated transistor and an enhancement-mode ion-gated transistor. h) The ion-gated transistor-based nonlinear rectifier provides high signal-to-noise real-time detection of epileptic discharges. Reproduced with permission.[130] Copyright 2020, Springer Nature.

stability was retained under continuous operation. Additionally, the authors created a voltage amplifier and confirmed the amplified signals using an OECT circuitry operated in the subthreshold region by measuring alpha rhythm activity between eyes closed and open (Figure 4e). Furthermore, the integration of different devices to increase the performance or provide new functionality to the device is an emerging topic.[15,19,130] Among these devices, slow response time and low signal-to-noise ratio have been obstacles to following up the frequency of biosignals and differentiating meaningful signals. However, this has been solved by developing enhancement-mode PEDOT:PSS with a very fast response time using ion-gated OECT (Figure 4f).[130] The resulting device was integrated with conventional depletion-mode PEDOT:PSS OECTs to form a nonlinear signal rectification circuit (Figure 4g). As a result, the authors succeeded in measuring several epileptic discharge signals that were transformed into easily detectable peaks by the ion-gated OECT circuit (Figure 4h).

5. Prerequisites for Biomedical Applications: Performance and Stability

Low power consumption, high sensitivity, stability in aqueous electrolytes, and biological and mechanical compatibility with living tissues are the advantages that OECTs have over other electronics for a variety of biomedical applications.[96,115,131–135] In particular, electrochemical transistors are expected to be

highly useful in biomolecule sensors and electroactive signal recording systems for their amplification and switching functions, which are inherent functions of transistors. In other words, the channel materials for the OECT satisfy the conditions mentioned above, high switching speed, high transconductance, and low impedance even when the OECT is used in electroactive signal recording, which is sensitive to the electroactive frequency of a cell. In addition, because biomedical devices are driven under repetitive driving or in-body electrolyte conditions, and water uptake or penetration of ions is inevitable,[29,136,137] the distortion of the resulting molecular arrangement can affect the performance and, ultimately, the operational stability of the device.[24,30,138] Therefore, this section discusses the prerequisites for channel materials of OECTs in biomedical applications and introduces the application of OECTs using various mixed conductors, including PEDOT:PSS.

5.1. Biocompatibility

In practice, the biocompatibility of materials is very ambiguous because the required properties and biocompatibility criteria depend on the materials used and applications.[141–144] For example, when a material is applied to an in vitro cell culture scaffold, the toxicity of the material and viability test of the cell are sufficient for biocompatibility evaluation.[145–147] However, for an in vivo cell culture scaffold, the reaction with the immune system and biodegradability of materials should be considered.[148–150] Furthermore, if the material is used for deep brain stimulation, it should be electrically insulated except for the part used to create the electrical signal.[151–153] This is crucial for stimulating only the desired site and the immune response of the material. The material can then be declared biocompatible with the application if all these biocompatibility evaluations are conducted with appropriate negative and positive controls. Therefore, a versatile biocompatibility evaluation method cannot exist, and the biocompatibility of the material should be evaluated by adjusting the scope according to the applications. However, in terms of stable device operation in the body, it is possible to set approximate criteria, such as the presence of cytotoxicity in the material used, viability of the cell upon cell contact with the device, and possibility of device degradation by an immune reaction.

5.2. Mixed Conductivity and Low Impedance

OECTs are primarily used for amplification and switching in biomedical applications, and these characteristics are determined by the transconductance of the device. The transconductance (g_m) of a device is defined as follows:

$$g_m = \frac{\partial I_D}{\partial V_G} = \frac{W}{L} d\mu C^* (V_T - V_G) \quad (1)$$

where I_D is the drain current, V_G is the gate voltage, d is the film thickness, μ is the charge carrier mobility, C^* is the volumetric capacitance, and V_T is the threshold voltage. The gate electric field is applied through a gate electrode, electrolyte, channel, and source; hence, it is vertically applied to the channel. The lateral I_D flowing through the drain, channel, and source is modulated by the V_G. In that sense, the lateral channel conductivity and transport characteristics of the electrolyte and channel are the primary factors for a higher g_m, and these are directly related to the electronic and ionic conductivities of the channel, respectively. In a biomolecular sensor, I_D modulation with different analyte concentrations is achieved by the electrochemical process of analytes in electrolytes affecting the conductivity of the channel.[7,11,13,14] Thus, the ions in electrolytes should penetrate the bulk of the channel during the process to change its conductivity; therefore, the ionic conductivity of the channel is related to the efficiency of this process. This is more evident in electroactive signal recorders because the electricity generated by electroactive cells is created by the ion flux at the cell wall. I_D is simply created by the charge carrier transport through the channel; therefore, the electrical conductivity of the channel consisting of the charge carrier density, elementary charge of the electron, and μ is important. However, as mentioned above, the charge carrier density is determined by V_G. Therefore, the ion conductivity and the mobility of the channel are the main factors. The aforementioned conductivity is related to direct current; the conductive or resistive component to alternating currents is also an important variable in the recording of electroactive signals in cells because neurons generate alternating electroactive signals called "spikes."[142,154,155] A low impedance is one of the advantages of a conductive polymer-based electrochemical transistor as a signal recording system compared with an electrolyte gate transistor.[158–160] As a high signal-to-noise ratio is the required characteristic of a signal recording system, a conductive polymer with a low impedance can be employed to record an electrical signal with a low noise ratio, and very fine signals can be detected.

5.3. Device Stability

Contact with body electrolytes and the cellular matrix are inevitable for OECTs employed for biomedical purposes; thus, the biocompatibility, electrical, and electrochemical properties of the channel, such as electronic and ionic conductivities, capacitance, reversible redox reaction, and carrier concentration, should be retained. Except for conductive polymers functionalized by glycol side chains, conductive polymers doped by polyelectrolytes have been widely used for OECTs because the ionic functional groups increase the solubility of the material. This means that the polymer film can be prepared through facile solution processes. However, ionic functional groups can result in protons and ions leaching out into the solvent; thus, the inherent properties of materials can be changed in electrolyte conditions.[161–163] This could be a critical disadvantage of OECTs for biomedical purposes. Therefore, the development of highly stable materials under electrolyte conditions is required. Meanwhile, for devices implanted for the diagnosis or treatment of chronic diseases, the operational stability of the device should be guaranteed because a repetitive gate bias would be applied to the device during implantation. Specifically, a repetitive gate bias causes ions to repeatedly enter and exit the vicinity of the polymer chains. This can also affect the long-term stability of the ion or electron conductivity of the channel by preventing the polymer chain from being fixed at one location. Therefore,

developing a material with the two above-mentioned stabilities is essential for biomedical applications that can best utilize an electrochemical transistor with the advantage of mixed conductivity.

6. Understanding the Structure–Property Relationship of Polymeric Mixed Conductors to Increase Device Performance and Stability

6.1. Ion-Permeable Polymeric Mixed Conductors

In the sections above, we provided an overview of organic electrochemical transistors and their active materials and applications. Hereafter, the structure–property relationships will be discussed in terms of molecular and material shapes. In thin-film transistors, the intrinsic parameters that determine performance are the charge carrier mobility (μ) and capacitance (C). The high capacitance value of a polymeric mixed conductor due to ion permeability (i.e., volumetric capacitance, C^*) is the most important factor distinguishing it from other semiconductors.[22] Therefore, the abovementioned parameters must be improved with reversible operations to develop high-performance electrochemical transistors. In inorganic semiconductors, where the atoms are tightly bonded to each other by covalent interaction, the ion cannot penetrate the channel; hence, the ion can only interact with the semiconductor on their surface (**Scheme 3**a).[164] For conjugated polymers, the covalently bonded chains adhere to each other loosely through van der Waals interactions, so they can provide a small space for ions to penetrate channels but still cannot support ionic transport into the volume (Scheme 3b).[165] Therefore, hydrophilic parts such as side chains or polyelectrolytes should be incorporated into the materials to enable ion transport through these parts (Scheme 3c,d).[134] On the other hand, recent studies reported that the unobstructed ion conduction hinders the electronic charge transport in OECTs. The repetitive injection of dopant ions into the mixed conductor channel deforms the film crystalline structure,[28,166] and this kind of phenomena depend on the size of ions and the amount of water molecules surrounding injected ions.[136,167] Flagg et al. demonstrated that the swelling of mixed conductor disturbs connections among crystalline domains, leading to the reduced carrier mobility in resultant OECTs.[29] These studies suggest that the performance of OECT can be optimized by balancing the corresponding ionic and electronic conductivities. Furthermore, the polymeric mixed conductors should be designed with a wide range of considerations, from the molecular level to the bulk channel morphology, to ensure high performance and robust stability.

6.2. Molecular Structures

As organic electrochemical transistors have attracted much interest owing to their potential for biomedical applications, conjugated polymers decorated with hydrophilic sidechains have been extensively reported to enable ions to access bulk materials and exhibit high-performance parameters.[49,50] In these studies, glycolic or hydroxyl sidechains were employed to introduce the pathways to ions, and sulfonic acid sidechains were employed to introduce hole doping and ion pathways (Scheme 3c and **Figure 5**a).[49,50,168] While ion-impermeable semiconductors maintained their absorption spectra regardless of the applied electrochemical potential, they exhibited dramatic changes in the spectra, which were due to volumetric charge accumulation (Figure 5b). In these molecular-level approaches, the chemical and physical properties of materials such as the operating voltages, doping states, ionic permeability, and crystallinity can be extensively tuned by controlling the types and length of sidechains. However, introducing excessively long glycolic chains can decrease both charge mobility and capacitance by hindering interchain charge transport, decreasing chain density, and inducing large swelling of channel materials, which results in channel degradation and delamination.[169] In

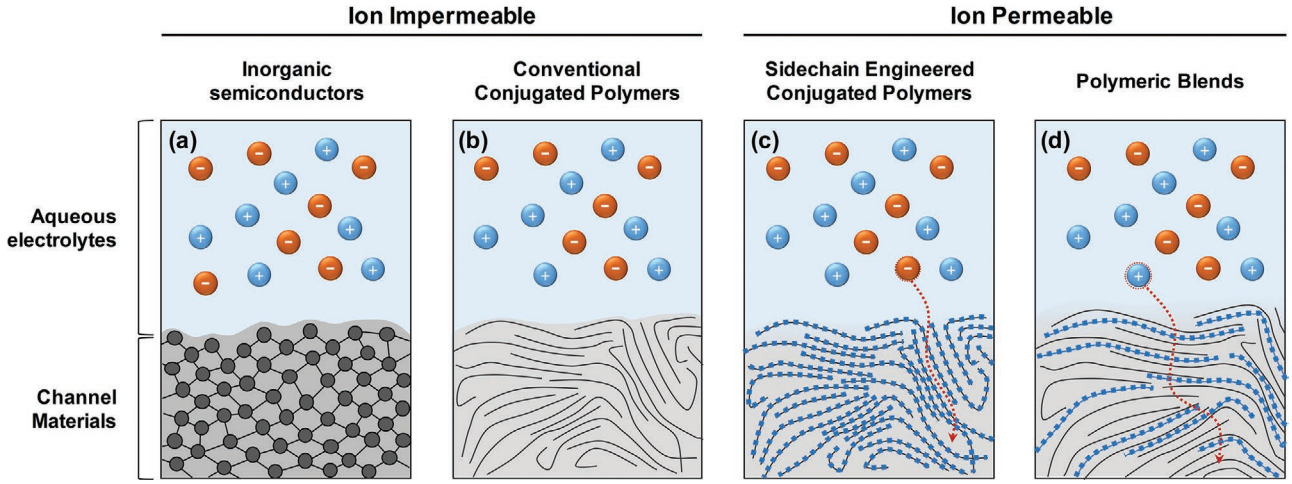

Scheme 3. Schematics of ion-impermeable and ion-permeable conductors at the aqueous electrolyte–channel interface. a) Inorganic semiconductors with tight covalent bonds between atoms. b) Conventional conjugated polymers such as P3HT with loose van der Waals bonds. c) Conjugated polymers decorated with hydrophilic side chains. d) Conjugated polymer blends with polyelectrolytes. Water-permeable moieties such as hydrophilic side chains and polyelectrolytes aid ions to penetrate the channel upon gate bias application.

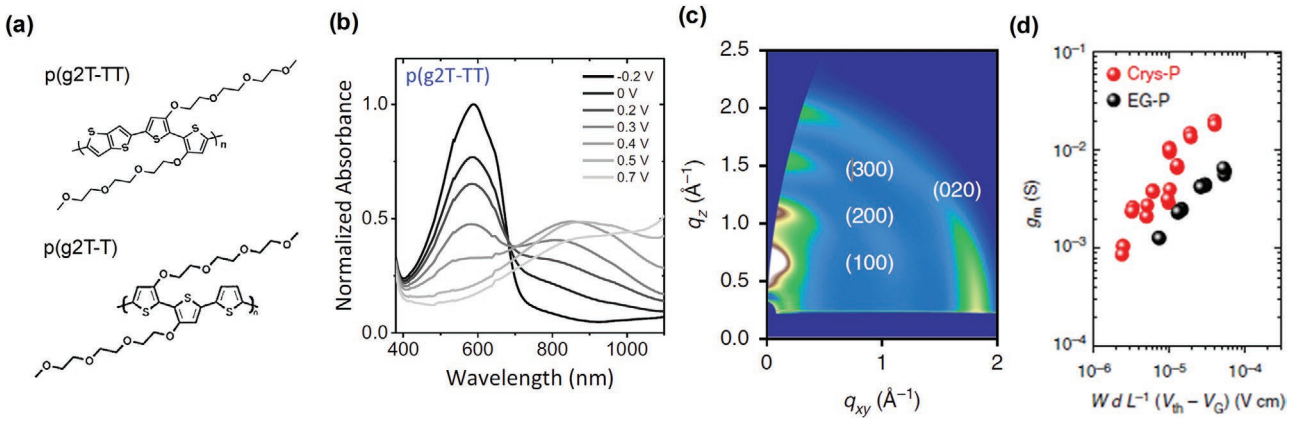

Figure 5. Ion-permeable conjugated systems. a) Chemical structures of p(g2T-TT) and p(g2T-T) polymers. b) Absorbance spectra of p(g2T-TT) films depending on the applied electrochemical potentials. Reproduced under the terms of Creative Commons Attribution 4.0 International License.[49] Copyright 2016, The Authors, published by National Academy of Sciences. c) Grazing incidence wide-angle X-ray scattering pattern for crystallized PEDOT:PSS. d) Transconductance (g_m) plot of crystallized PEDOT:PSS and ethylene glycol-treated PEDOT:PSS as a function of the applied gate bias and channel geometry. Reproduced under the terms of Creative Commons Attribution 4.0 International License.[28] Copyright 2018, The Authors, published by Springer Nature.

addition, chain entanglement and addition of crosslinkers can increase the mechanical properties of channels, which can increase film stability by resisting film swelling effects.[170]

6.3. Polymer Blending Structures

The blending of hydrophilic polymers with conjugated polymers can enable ions to access the channels. PEDOT:PSS, in which PEDOT chains are mixed with PSS chains in the entire material, is a common polymeric blend frequently employed as a mixed conductor. As charge carrier pathways of PEDOT coexist in the channel with ionic pathways of PSS, the ions and electrons can efficiently transport through these electronic and ionic transport pathways (Scheme 3d). However, if more hydrophilic polymers than is necessary for enabling ionic transport are incorporated in the blending, such polymers can lead to a decrease in both device performance and stability by interfering with the inter-chain transport of the charge carriers and increase channel swelling at aqueous interfaces.

In practice, the commercially available stable aqueous dispersion of PEDOT:PSS has an approximately twice as high an amount of PSS than PEDOT; hence, this blend is formed as a granular domain in which PEDOT chains are wrapped with PSS-rich shells. Therefore, PEDOT:PSS cannot be expected to have high electrical conductivity without the aid of additional chemicals. Furthermore, even with chemical addition, charge and ionic mobilities have a trade-off relationship, which results in the saturation of performance parameters.[26] However, when the excess PSS is removed through the post-treatment of PEDOT:PSS, PEDOT chains are significantly aligned in the edge-on direction, and chains form porous morphologies (Figure 5c). Moreover, crystallized PEDOT:PSS exhibited a performance five times higher than that of other PEDOT:PSS films and stable performance even after 21 days of water immersion (Figure 5d).[28] As a result of removing excess PSS, aligned PEDOT chains can afford better electronic pathways for charge carriers, nanoscale pores can act as augmented pathways for ion transport, and the swelling at aqueous interfaces can be attenuated. Therefore, the types and amounts of polyelectrolytes blended with conjugated polymers should be carefully controlled to achieve high performance and stability.

6.4. Bulk Morphology

The bulk channel morphology can affect the performance and stability of OECTs. Generally, in the typical operation of thin-film transistors, ions can only penetrate in the vertical direction of the device configuration, making it more difficult for ions to reach the bottom part of the films as the thickness of the channel increases (**Figure 6**a,b). Meanwhile, if microfiber-shaped conjugated polymer channels are employed, ions can penetrate the channel in all radial directions, promoting ionic transport in a morphological manner (Figure 6c,d). Additionally, a freestanding form of microfiber can comply with dimensional changes caused by swelling; hence, providing higher mechanical stability of channels.[171] In terms of device fabrication, microfibers can offer a wide range of channel thickness from sub-micrometers to tens of micrometers through wet-spinning; thus, channel dimensions can be extremely adjusted to extremes, depending on the purpose. Therefore, a transistor configuration with freestanding microfibers is more favorable for providing more efficient ionic transport and mechanical stability of the channel.

7. Outlook

In the sections above, we focused on the principles, materials, and detailed use of bioelectronic devices throughout the field and clearly provided the requirements for materials used in bioelectronic devices. The mixed conductivity, mechanical flexibility, volumetric capacitance, and processability of a material are essential characteristics for the high performance and stability of bioelectronic devices. Hence, a polymeric material with

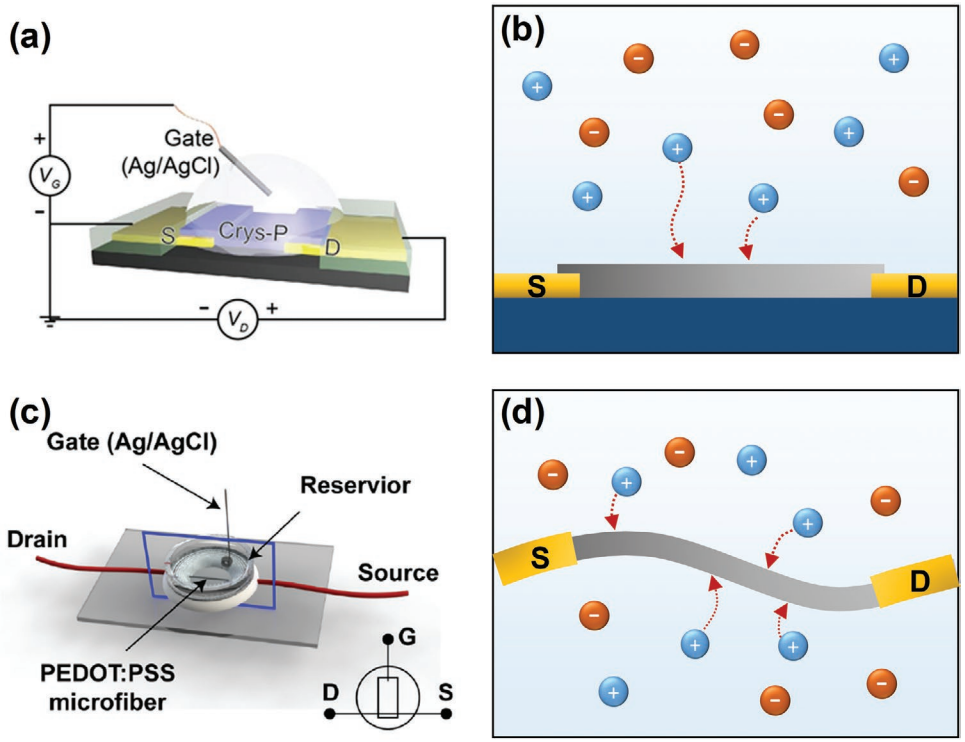

Figure 6. Graphical descriptions of ionic transport in organic electrochemical transistors. a) Typical thin-film organic electrochemical transistor configuration. Reproduced under the terms of Creative Commons Attribution 4.0 International License.[28] Copyright 2018, The Authors, published by Springer Nature. b) Cross-sectional graphic describing ion transport into the thin-film channel. c) Wet-spun microfiber-based electrochemical transistor configuration and ionic transport. Reproduced under the terms of Creative Commons Attribution 4.0 International License.[171] Copyright 2018, The Authors, published by Springer Nature. d) Ionic transport in microfiber-based transistors.

mixed conductivity has a superior advantage over inorganic materials in terms of transconductance, signal-to-noise ratio, and impedance. Above all, the ease of functionalization distinguishes polymeric mixed conductors from inorganic materials in that they can facilitate the design of the structure and properties of the material according to the intended use, which was the primary reason for discussing the design of polymeric mixed conductors in this review. Therefore, it is expected that OECTs using polymeric mixed conductors can be used for the detection and measurement of biological information and in the field of bioelectronics, such as in ion injection and long-term stimulation using artificial electrical signals. However, some unknown principles and problems remain to be solved for polymeric mixed conductors; thus, the materials currently used have limitations. In this section, we present the directions to be investigated and discuss the prospects of organic electrochemical transistors based on them.

7.1. Enhancing Carrier Mobility and Stability

Due to the nature of polymeric materials with irregular molecular arrangements, achieving high hole-transporting characteristics is difficult, which is considered to be a typical limitation of organic materials compared with inorganic materials. Another difficulty is the stability problem. As mentioned earlier, the repetitive entry and exit of ions can destroy the molecular arrangement and degrade the properties of the material and the performance of the device. A common feature of these two problems is that each property is deeply related to the arrangement of molecules, and the more regular the molecule arrangement, the better the hole transfer characteristics and stability. Therefore, the performance and stability of the OECT can be effectively increased by enhancing the crystallinity of the polymeric material used as the channel. For PEDOT:PSS, a typical polymeric mixed conductor, many studies have been conducted on the improvement of the crystallinity and its effect has been proved. However, because this approach is relatively insufficient for other kinds of polymeric materials, studies on the crystallinity of materials such as p(g2T-TT), g2T-TT, and p(gNDI-gT2), which are currently being developed, and on the structural and process design of polymers considering these materials are expected to provide a solution that can increase the overall performance and stability of OECTs.

7.2. Nonaqueous Device Operation

Although mixed conductors have many advantages, such as high capacitance and ease of large-scale fabrication, a significant constraint is that mixed conductors can be properly operated only when a sufficient number of ions interact with the conjugated system. Thus, the device can generally and frequently be operated in aqueous electrolytes, but it can only be employed to measure bioelectric signals from wet tissues or biochemical signals from aqueous samples, which means that

the device should be implanted in the target tissue to measure bioelectric signals. Meanwhile, skin electronics have attracted considerable interest owing to their mechanical conformability and capability to measure biosignals noninvasively. Indeed, as a bioelectric sensor is less invasive, it can be used for wider field applications in medical devices, cosmetics, and in general healthcare devices. Therefore, prompt efforts to develop dry organic mixed conductors to provide alternative ion species to conjugated systems as substitutes for aqueous electrolytes are necessary.

7.3. Introduction of Functional Groups

As the introduction of glycol side chains or ionic functional groups into the ion-impermeable semiconducting conjugated polymer opens new prospects for accumulation-mode OECTs, the introduction of functional groups to the polymeric mixed conductor may be an opportunity for new applications. For instance, covalently cross-linked porous 3D scaffolds using functional PEDOT (f-PEDOT) have been reported.[172] A significantly large f-PEDOT hydrogel was obtained (up to 402 mm^3, swollen in water), and the suitability of the hydrogel as a 3D cell culture scaffold was demonstrated. Another option may be to replace the dopant of polyelectrolyte-doped conjugated polymers with biopolymers. The acidity of PSS in PEDOT:PSS is well-known and it would not be appropriate for some biomedical applications; thus, a suitable biocompatible dopant material can increase both performance and biocompatibility. Lignosulfonate, which can be prepared through the sulfonation of lignin, the second most abundant biopolymer, can act both as a dopant and dispersing agent as PSS for PEDOT:PSS.[173] PEDOT doped with lignin (PEDOT/lig) doubles the specific capacitance compared with PEDOT:PSS, which is attributed to the additional pseudocapacitance generated by the quinone moieties in lignin. Similarly, another functionality can be introduced to the polymeric mixed conductors and provide new opportunities for biomedical devices because there are many biomolecules of interest in our body system and unknown, complicated systems in neural networks that require study.

8. Conclusions

In summary, there have been dramatic advances in the understanding of using polymeric mixed conductors for OECTs, as evidenced by the deep understanding of the region related to ion and electron conduction and creatively designed materials for biomedical applications. Based on the understanding of the ion and electron conduction of PEDOT:PSS, which is a typical channel material of OECTs, many polymeric mixed conductors have been developed. Through analysis of it as transistor channel material, and various methods to satisfy the requirements of biomolecular sensors and electroactive signal recorders, the key variables related to the performance and stability of the device were identified. The structural design of the polymeric mixed conductor is key to improving both the performance and stability, as demonstrated in several studies that focus on the crystallinity and geometrical differences of various devices and channel materials. Furthermore, an outlook on future polymeric mixed conductors and OECTs was suggested, which emanates from the abovementioned property–performance relationship. We believe that these prospects and challenges will eventually become new opportunities for future endeavors that this article attempts to encourage and that multifunctional OECTs based on diverse polymeric mixed conductors will have a competitive edge in a range of future bioelectronics.

Acknowledgements

J.H.K. and S.-M.K. contributed equally to this work. This work was supported by the Basic Science Research Program through the National Research Foundation of Korea (NRF) funded by the Ministry of Science and ICT (NRF-2020M3D1A1030660 and NRF-2018M3A7B4070988) and by GIST Research Institute (GRI) grant funded by the GIST in 2020.

Conflict of Interest

The authors declare no conflict of interest.

Keywords

biosensors, mixed conductors, organic electrochemical transistors, structures and properties

Received: June 18, 2020
Revised: August 11, 2020
Published online:

[1] D. Khodagholy, J. Rivnay, M. Sessolo, M. Gurfinkel, P. Leleux, L. H. Jimison, E. Stavrinidou, T. Herve, S. Sanaur, R. M. Owens, G. G. Malliaras, *Nat. Commun.* **2013**, *4*, 2133.
[2] J. Rivnay, P. Leleux, M. Sessolo, D. Khodagholy, T. Hervé, M. Fiocchi, G. G. Malliaras, *Adv. Mater.* **2013**, *25*, 7010.
[3] S. Inal, J. Rivnay, P. Leleux, M. Ferro, M. Ramuz, J. C. Brendel, M. M. Schmidt, M. Thelakkat, G. G. Malliaras, *Adv. Mater.* **2014**, *26*, 7450.
[4] P. Gkoupidenis, N. Schaefer, B. Garlan, G. G. Malliaras, *Adv. Mater.* **2015**, *27*, 7176.
[5] Y. van de Burgt, E. Lubberman, E. J. Fuller, S. T. Keene, G. C. Faria, S. Agarwal, M. J. Marinella, A. Alec Talin, A. Salleo, *Nat. Mater.* **2017**, *16*, 414.
[6] P. Gkoupidenis, D. A. Koutsouras, G. G. Malliaras, *Nat. Commun.* **2017**, *8*, 15448.
[7] A. M. Pappa, D. Ohayon, A. Giovannitti, I. P. Maria, A. Savva, I. Uguz, J. Rivnay, I. McCulloch, R. M. Owens, S. Inal, *Sci. Adv.* **2018**, *4*, eaat0911.
[8] X. Strakosas, M. Huerta, M. J. Donahue, A. Hama, A.-M. Pappa, M. Ferro, M. Ramuz, J. Rivnay, R. M. Owens, *J. Appl. Polym. Sci.* **2016**, *134*, 44483.
[9] M. Braendlein, A.-M. Pappa, M. Ferro, A. Lopresti, C. Acquaviva, E. Mamessier, G. G. Malliaras, R. M. Owens, *Adv. Mater.* **2017**, *29*, 1605744.
[10] A.-M. Pappa, V. F. Curto, M. Braendlein, X. Strakosas, M. J. Donahue, M. Fiocchi, G. G. Malliaras, R. M. Owens, *Adv. Healthcare Mater.* **2016**, *5*, 2295.

[11] E. Bihar, Y. Deng, T. Miyake, M. Saadaoui, G. G. Malliaras, M. Rolandi, *Sci. Rep.* **2016**, *6*, 27582.
[12] M. E. Welch, T. Doublet, C. Bernard, G. G. Malliaras, C. K. Ober, *J. Polym. Sci., Part A: Polym. Chem.* **2015**, *53*, 372.
[13] D. Khodagholy, V. F. Curto, K. J. Fraser, M. Gurfinkel, R. Byrne, D. Diamond, G. G. Malliaras, F. Benito-Lopez, R. M. Owens, *J. Mater. Chem.* **2012**, *22*, 4440.
[14] S. Wustoni, A. Savva, R. Sun, E. Bihar, S. Inal, *Adv. Mater. Interfaces* **2019**, *6*, 1800928.
[15] C. M. Proctor, I. Uguz, A. Slezia, V. Curto, S. Inal, A. Williamson, G. G. Malliaras, *Adv. Biosyst.* **2019**, *3*, 1800270.
[16] A. Jonsson, S. Inal, I. Uguz, A. J. Williamson, L. Kergoat, J. Rivnay, D. Khodagholy, M. Berggren, C. Bernard, G. G. Malliaras, D. T. Simon, *Proc. Natl. Acad. Sci. USA* **2016**, *113*, 9440.
[17] W. Lee, S. Kobayashi, M. Nagase, Y. Jimbo, I. Saito, Y. Inoue, T. Yambe, M. Sekino, G. G. Malliaras, T. Yokota, M. Tanaka, T. Someya, *Sci. Adv.* **2018**, *4*, eaau2426.
[18] W. Lee, D. Kim, N. Matsuhisa, M. Nagase, M. Sekino, G. G. Malliaras, T. Yokota, T. Someya, *Proc. Natl. Acad. Sci. USA* **2017**, *40*, 201703886.
[19] W. Lee, D. Kim, J. Rivnay, N. Matsuhisa, T. Lonjaret, T. Yokota, H. Yawo, M. Sekino, G. G. Malliaras, T. Someya, *Adv. Mater.* **2016**, *28*, 9722.
[20] A. Williamson, M. Ferro, P. Leleux, E. Ismailova, A. Kaszas, T. Doublet, P. Quilichini, J. Rivnay, B. Rózsa, G. Katona, C. Bernard, G. G. Malliaras, *Adv. Mater.* **2015**, *27*, 4405.
[21] D. Khodagholy, T. Doublet, P. Quilichini, M. Gurfinkel, P. Leleux, A. Ghestem, E. Ismailova, T. Hervé, S. Sanaur, C. Bernard, G. G. Malliaras, *Nat. Commun.* **2013**, *4*, 1575.
[22] J. Rivnay, P. Leleux, M. Ferro, M. Sessolo, A. Williamson, D. A. Koutsouras, D. Khodagholy, M. Ramuz, X. Strakosas, R. M. Owens, C. Benar, J.-M. Badier, C. Bernard, G. G. Malliaras, *Sci. Adv.* **2015**, *1*, e1400251.
[23] M. Moser, T. C. Hidalgo, J. Surgailis, J. Gladisch, S. Ghosh, R. Sheelamanthula, Q. Thiburce, A. Giovannitti, A. Salleo, N. Gasparini, A. Wadsworth, I. Zozoulenko, M. Berggren, E. Stavirinidou, S. Inal, I. McCulloch, *Adv. Mater.* **2020**, 2002748 https://doi.org/10.1002/adma.202002748.
[24] N. Rolland, J. F. Franco-Gonzalez, R. Volpi, M. Linares, I. V. Zozoulenko, *Phys. Rev. Mater.* **2018**, *2*, 045605.
[25] R. Noriega, J. Rivnay, K. Vandewal, F. P. V. Koch, N. Stingelin, P. Smith, M. F. Toney, A. Salleo, *Nat. Mater.* **2013**, *12*, 1038.
[26] J. Rivnay, S. Inal, B. A. Collins, M. Sessolo, E. Stavrinidou, X. Strakosas, C. Tassone, D. M. Delongchamp, G. G. Malliaras, *Nat. Commun.* **2016**, *7*, 11287.
[27] J. T. Friedlein, J. Rivnay, D. H. Dunlap, I. McCulloch, S. E. Shaheen, R. R. McLeod, G. G. Malliaras, *Appl. Phys. Lett.* **2017**, *111*, 023301.
[28] S.-M. Kim, C.-H. Kim, Y. Kim, N. Kim, W.-J. Lee, E.-H. Lee, D. Kim, S. Park, K. Lee, J. Rivnay, M.-H. Yoon, *Nat. Commun.* **2018**, *9*, 3858.
[29] L. Q. Flagg, C. G. Bischak, J. W. Onorato, R. B. Rashid, C. K. Luscombe, D. S. Ginger, *J. Am. Chem. Soc.* **2019**, *141*, 4345.
[30] J. O. Guardado, A. Salleo, *Adv. Funct. Mater.* **2017**, *27*, 1701791.
[31] H. Sirringhaus, P. J. Brown, R. H. Friend, M. M. Nielsen, K. Bechgaard, B. M. W. Langeveld-Voss, A. J. H. Spiering, R. a. J. Janssen, E. W. Meijer, P. Herwig, D. M. de Leeuw, *Nature* **1999**, *401*, 685.
[32] M. Moser, J. F. Ponder, A. Wadsworth, A. Giovannitti, I. McCulloch, *Adv. Funct. Mater.* **2019**, *29*, 1807033.
[33] E. Zeglio, O. Inganäs, *Adv. Mater.* **2018**, *30*, 1800941.
[34] S. Inal, J. Rivnay, A.-O. Suiu, G. G. Malliaras, I. McCulloch, *Acc. Chem. Res.* **2018**, *51*, 1368.
[35] J. T. Friedlein, R. R. McLeod, J. Rivnay, *Org. Electron.* **2018**, *63*, 398.
[36] M. J. Panzer, C. D. Frisbie, *J. Am. Chem. Soc.* **2007**, *129*, 6599.
[37] L. Kergoat, L. Herlogsson, B. Piro, M. C. Pham, G. Horowitz, X. Crispin, M. Berggren, *Proc. Natl. Acad. Sci. USA* **2012**, *109*, 8394.
[38] B. Nketia-Yawson, S.-J. Kang, G. D. Tabi, A. Perinot, M. Caironi, A. Facchetti, Y.-Y. Noh, *Adv. Mater.* **2017**, *29*, 1605685.
[39] F. Leonardi, S. Casalini, Q. Zhang, S. Galindo, D. Gutierrez, M. Mas-Torrent, *Adv. Mater.* **2016**, *28*, 10311.
[40] O. Larsson, A. Laiho, W. Schmickler, M. Berggren, X. Crispin, *Adv. Mater.* **2011**, *23*, 4764.
[41] A. Laiho, L. Herlogsson, R. Forchheimer, X. Crispin, M. Berggren, *Proc. Natl. Acad. Sci. USA* **2011**, *108*, 15069.
[42] J. Lee, L. G. Kaake, J. H. Cho, X.-Y. Zhu, T. P. Lodge, C. D. Frisbie, *J. Phys. Chem. C* **2009**, *113*, 8972.
[43] L. Herlogsson, X. Crispin, N. D. Robinson, M. Sandberg, O.-J. Hagel, G. Gustafsson, M. Berggren, *Adv. Mater.* **2007**, *19*, 97.
[44] E. Said, X. Crispin, L. Herlogsson, S. Elhag, N. D. Robinson, M. Berggren, *Appl. Phys. Lett.* **2006**, *89*, 143507.
[45] E. Zeglio, M. Vagin, C. Musumeci, F. N. Ajjan, R. Gabrielsson, X. T. Trinh, N. T. Son, A. Maziz, N. Solin, O. Inganäs, *Chem. Mater.* **2015**, *27*, 6385.
[46] S. Inal, J. Rivnay, A. I. Hofmann, I. Uguz, M. Mumtaz, D. Katsigiannopoulos, C. Brochon, E. Cloutet, G. Hadziioannou, G. G. Malliaras, *J. Polym. Sci., Part B: Polym. Phys.* **2016**, *54*, 147.
[47] E. Zeglio, J. Eriksson, R. Gabrielsson, N. Solin, O. Inganäs, *Adv. Mater.* **2017**, *29*, 1605787.
[48] E. Zeglio, M. M. Schmidt, M. Thelakkat, R. Gabrielsson, N. Solin, O. Inganäs, *Chem. Mater.* **2017**, *29*, 4293.
[49] A. Giovannitti, D.-T. Sbircea, S. Inal, C. B. Nielsen, E. Bandiello, D. A. Hanifi, M. Sessolo, G. G. Malliaras, I. McCulloch, J. Rivnay, *Proc. Natl. Acad. Sci. USA* **2016**, *113*, 12017.
[50] C. B. Nielsen, A. Giovannitti, D.-T. Sbircea, E. Bandiello, M. R. Niazi, D. A. Hanifi, M. Sessolo, A. Amassian, G. G. Malliaras, J. Rivnay, I. McCulloch, *J. Am. Chem. Soc.* **2016**, *138*, 10252.
[51] L. R. Savagian, A. M. Österholm, J. F. Ponder, K. J. Barth, J. Rivnay, J. R. Reynolds, *Adv. Mater.* **2018**, *30*, 1804647.
[52] F. Buth, A. Donner, M. Sachsenhouser, M. Stutzmann, J. A. Garride, *Adv. Mater.* **2012**, *24*, 4511.
[53] J. C. Lassegues, J. Grondin, T. Becker, L. Servant, M. Hernandez, *Solid State Ion* **1995**, *77*, 311.
[54] G. Tarabella, C. Santato, S. Y. Yang, S. Iannotta, G. G. Malliaras, F. Cicoira, *Appl. Phys. Lett.* **2010**, *97*, 123304.
[55] E. Stavrinidou, P. Leleux, H. Rajaona, D. Khodagholy, J. Rivnay, M. Lindau, S. Sanaur, G. G. Malliaras, *Adv. Mater.* **2013**, *25*, 4488.
[56] P. Kumar, Z. Yi, S. Zhang, S. Sekar, F. Soavi, F. Cicoira, *Appl. Phys. Lett.* **2015**, *107*, 053303.
[57] P.-O. Svensson, D. Nilsson, R. Forchheimer, M. Berggren, *Appl. Phys. Lett.* **2008**, *93*, 203301.
[58] H. Toss, C. Suspène, B. Piro, A. Yassar, X. Crispin, L. Kergoat, M.-C. Pham, M. Berggren, *Org. Electron.* **2014**, *15*, 2420.
[59] P. Andersson Ersman, D. Nilsson, J. Kawahara, G. Gustafsson, M. Berggren, *Org. Electron.* **2013**, *14*, 1276.
[60] H. Tang, P. Kumar, S. Zhang, Z. Yi, G. D. Crescenzo, C. Santato, F. Soavi, F. Cicoira, *ACS Appl. Mater. Interfaces* **2015**, *7*, 969.
[61] G. C. Faria, D. T. Duong, A. Salleo, *Org. Electron.* **2017**, *45*, 215.
[62] N. Kim, H. Kang, J.-H. Lee, S. Kee, S. H. Lee, K. Lee, *Adv. Mater.* **2015**, *27*, 2317.
[63] Y. Xia, J. Ouyang, *ACS Appl. Mater. Interfaces* **2012**, *4*, 4131.
[64] Y. Xia, K. Sun, J. Ouyang, *Energy Environ. Sci.* **2012**, *5*, 5325.
[65] D. Alemu, H.-Y. Wei, K.-C. Ho, C.-W. Chu, *Energy Environ. Sci.* **2012**, *5*, 9662.
[66] C. Badre, L. Marquant, A. M. Alsayed, L. A. Hough, *Adv. Funct. Mater.* **2012**, *22*, 2723.
[67] M. V. Fabretto, D. R. Evans, M. Mueller, K. Zuber, P. Hojati-Talemi, R. D. Short, G. G. Wallace, P. J. Murphy, *Chem. Mater.* **2012**, *24*, 3998.
[68] S. Mukherjee, R. Singh, S. Gopinathan, S. Murugan, S. Gawali, B. Saha, J. Biswas, S. Lodha, A. Kumar, *ACS Appl. Mater. Interfaces* **2014**, *6*, 17792.

[69] C. M. Palumbiny, C. Heller, C. J. Schaffer, V. Körstgens, G. Santoro, S. V. Roth, P. Müller-Buschbaum, *J. Phys. Chem. C* **2014**, *118*, 13598.
[70] T. Takano, H. Masunaga, A. Fujiwara, H. Okuzaki, T. Sasaki, *Macromolecules* **2012**, *45*, 3859.
[71] L. Groenendaal, F. Jonas, D. Freitag, H. Pielartzik, J. R. Reynolds, *Adv. Mater.* **2000**, *12*, 481.
[72] S. Kirchmeyer, K. Reuter, *J. Mater. Chem.* **2005**, *15*, 2077.
[73] K. Sun, S. Zhang, P. Li, Y. Xia, X. Zhang, D. Du, F. H. Isikgor, J. Ouyang, *J. Mater. Sci.: Mater. Electron.* **2015**, *26*, 4438.
[74] R. Yue, J. Xu, *Synth. Met.* **2012**, *162*, 912.
[75] J. Newman, K. E. Thomas-Alyea, *Electrochemical Systems*, Wiley, NJ **2004**.
[76] A. J. Heeger, N. S. Sariciftci, E. B. Namdas, *Semiconducting and Metallic Polymers*, Oxford University Press, Oxford **2010**.
[77] Y. H. Kim, C. Sachse, M. L. Machala, C. May, L. Müller-Meskamp, K. Leo, *Adv. Funct. Mater.* **2011**, *21*, 1076.
[78] J. P. Thomas, L. Zhao, D. McGillivray, K. T. Leung, *J. Mater. Chem. A* **2014**, *2*, 2383.
[79] Q. Wei, M. Mukaida, Y. Naitoh, T. Ishida, *Adv. Mater.* **2013**, *25*, 2831.
[80] N. Kim, S. Kee, S. H. Lee, B. H. Lee, Y. H. Kahng, Y.-R. Jo, B.-J. Kim, K. Lee, *Adv. Mater.* **2014**, *26*, 2268.
[81] J. E. McCarthy, C. A. Hanley, L. J. Brennan, V. G. Lambertini, Y. K. Gun'ko, *J. Mater. Chem. C* **2013**, *2*, 764.
[82] D. A. Mengistie, M. A. Ibrahem, P.-C. Wang, C.-W. Chu, *ACS Appl. Mater. Interfaces* **2014**, *6*, 2292.
[83] Y. Xia, K. Sun, J. Ouyang, *Adv. Mater.* **2012**, *24*, 2436.
[84] M. A. Ratner, D. F. Shriver, *Chem. Rev.* **1988**, *88*, 109.
[85] A. Maitra, A. Heuer, *Phys. Rev. Lett.* **2007**, *98*, 227802.
[86] J. C. Dyre, P. Maass, B. Roling, D. L. Sidebottom, *Rep. Prog. Phys.* **2009**, *72*, 046501.
[87] K. I. S. Mongcopa, M. Tyagi, J. P. Mailoa, G. Samsonidze, B. Kozinsky, S. A. Mullin, D. A. Gribble, H. Watanabe, N. P. Balsara, *ACS Macro Lett.* **2018**, *7*, 504.
[88] V. Ganesan, V. Pyramitsyn, C. Bertoni, M. Shah, *ACS Macro Lett.* **2012**, *1*, 513.
[89] S. Inal, G. G. Malliaras, J. Rivnay, *Nat. Commun.* **2017**, *8*, 1767.
[90] S. Zhang, E. Hubis, C. Girard, P. Kumar, J. DeFranco, F. Cicoira, *J. Mater. Chem. C* **2016**, *4*, 1382.
[91] M. ElMahmoudy, S. Inal, A. Charrier, I. Uguz, G. G. Malliaras, S. Sanaur, *Macromol. Mater. Eng.* **2017**, *302*, 1600497.
[92] I. Uguz, M. Ganji, A. Hama, A. Tanaka, S. Inal, A. Youssef, R. M. Owens, P. P. Quilichini, A. Ghestem, C. Bernard, S. A. Dayeh, G. G. Malliaras, *Adv. Healthcare Mater.* **2016**, *5*, 3094.
[93] C. Yao, Q. Li, J. Guo, F. Yan, I.-M. Hsing, *Adv. Healthcare Mater.* **2015**, *4*, 528.
[94] P. Lin, X. Luo, I.-M. Hsing, F. Yan, *Adv. Mater.* **2011**, *23*, 4035.
[95] C. Liao, C. Mak, M. Zhang, H. L. W. Chan, F. Yan, *Adv. Mater.* **2015**, *27*, 676.
[96] Z. Yi, L. G. Bettini, G. Tomasello, P. Kumar, P. Piseri, I. Valitova, P. Milani, F. Soavi, F. Cicoira, *J. Polym. Sci., Part B: Polym. Phys.* **2017**, *55*, 96.
[97] Y. Ahn, Y. Jeong, Y. Lee, *ACS Appl. Mater. Interfaces* **2012**, *4*, 6410.
[98] H. Wu, L. Hu, M. W. Rowell, D. Kong, J. J. Cha, J. R. McDonough, J. Zhu, Y. Yang, M. D. McGehee, Y. Cui, *Nano Lett.* **2010**, *10*, 4242.
[99] J. L. Elechiguerra, L. Larios-Lopez, C. Liu, D. Garcia-Gutierrez, A. Camacho-Bragado, M. J. Yacaman, *Chem. Mater.* **2005**, *17*, 6042.
[100] J. P. Franey, G. W. Kammlott, T. E. Graedel, *Corros. Sci.* **1985**, *25*, 133.
[101] H. S. White, G. P. Kittlesen, M. S. Wrighton, *J. Am. Chem. Soc.* **1984**, *106*, 5375.
[102] E. W. Paul, A. J. Ricco, M. S. Wrighton, *J. Phys. Chem.* **1985**, *89*, 1441.
[103] G. Williams, H. N. McMurray, *Electrochem. Solid-State Lett.* **2005**, *8*, B42.
[104] J. D. Yuen, A. S. Dhoot, E. B. Namdas, N. E. Coates, M. Heeney, I. McCulloch, D. Moses, A. J. Heeger, *J. Am. Chem. Soc.* **2007**, *129*, 14367.
[105] S. Chao, M. S. Wrighton, *J. Am. Chem. Soc.* **1987**, *109*, 6627.
[106] O. Stéphan, P. Schottland, P.-Y. Le Gall, C. Chevrot, C. Mariet, M. Carrier, *J. Electroanal. Chem.* **1998**, *443*, 217.
[107] G. Zotti, S. Zecchin, G. Schiavon, L. 'Bert' Groenendaal, *Macromol. Chem. Phys.* **2002**, *203*, 1958.
[108] D. M. de Leeuw, M. M. J. Simenon, A. R. Brown, R. E. F. Einerhand, *Synth. Met.* **1997**, *87*, 53.
[109] D. Natali, M. Caironi, *Adv. Mater.* **2012**, *24*, 1357.
[110] A. Giovannitti, C. B. Nielsen, D.-T. Sbircea, S. Inal, M. Donahue, M. R. Niazi, D. A. Hanifi, A. Amassian, G. G. Malliaras, J. Rivnay, I. McCulloch, *Nat. Commun.* **2016**, *7*, 13066.
[111] H. Sun, M. Vagin, S. Wang, X. Crispin, R. Forchheimer, M. Berggren, S. Fabiano, *Adv. Mater.* **2018**, *30*, 1704916.
[112] S. Wang, H. Sun, U. Ail, M. Vagin, P. O. Å. Persson, J. W. Andreasen, W. Thiel, M. Berggren, X. Crispin, D. Fazzi, S. Fabiano, *Adv. Mater.* **2016**, *28*, 10764.
[113] Y. Liang, Z. Chen, Y. Jing, Y. Rong, A. Facchetti, Y. Yao, *J. Am. Chem. Soc.* **2015**, *137*, 4956.
[114] H. Tang, F. Yan, P. Lin, J. Xu, H. L. W. Chan, *Adv. Funct. Mater.* **2011**, *21*, 2264.
[115] D. A. Bernards, D. J. Macaya, M. Nikolou, J. A. DeFranco, S. Takamatsu, G. G. Malliaras, *J. Mater. Chem.* **2007**, *18*, 116.
[116] Y. Kim, J. Do, J. Kim, S. Y. Yang, G. G. Malliaras, C. K. Ober, E. Kim, *Jpn. J. Appl. Phys.* **2010**, *49*, 01AE10.
[117] P. N. Bartlett, *Analyst* **1998**, *123*, 387.
[118] S. Y. Yang, F. Cicoira, R. Byrne, F. Benito-Lopez, D. Diamond, R. M. Owens, G. G. Malliaras, *Chem. Commun.* **2010**, *46*, 7972.
[119] J. Liao, S. Lin, Y. Yang, K. Liu, W. Du, *Sens. Actuators, B* **2015**, *208*, 457.
[120] X. Ji, H. Y. Lau, X. Ren, B. Peng, P. Zhai, S.-P. Feng, P. K. L. Chan, *Adv. Mater. Technol.* **2016**, *1*, 1600042.
[121] Y. Fu, N. Wang, A. Yang, H. K. Law, L. Li, F. Yan, *Adv. Mater.* **2017**, *29*, 1703787.
[122] G. Somlo, S. K. Lau, P. Frankel, H. B. Hsieh, X. Liu, L. Yang, R. Krivacic, R. H. Bruce, *Breast Cancer Res. Treat.* **2011**, *128*, 155.
[123] A. Al-Ani, H. Pingle, N. P. Reynolds, P.-Y. Wang, P. Kingshott, *Polymers* **2017**, *9*, 343.
[124] S.-M. Kim, N. Kim, Y. Kim, M.-S. Baik, M. Yoo, D. Kim, W.-J. Lee, D.-H. Kang, S. Kim, K. Lee, M.-H. Yoon, *NPG Asia Mater.* **2018**, *10*, 255.
[125] D. C. Rodger, A. J. Fong, W. Li, H. Ameri, A. K. Ahuja, C. Gutierrez, I. Lavrov, H. Zhong, P. R. Menon, E. Meng, J. W. Burdick, R. R. Roy, V. R. Edgerton, J. D. Weiland, M. S. Humayun, Y.-C. Tai, *Sens. Actuators, B* **2008**, *132*, 449.
[126] M. E. Spira, A. Hai, *Nat. Nanotechnol.* **2013**, *8*, 83.
[127] V. Venkatraman, J. T. Friedlein, A. Giovannitti, I. P. Maria, I. McCulloch, R. R. McLeod, J. Rivnay, *Adv. Sci.* **2018**, *5*, 1800453.
[128] E. Vittoz, J. Fellrath, *IEEE J. Solid-State Circuits* **1977**, *12*, 224.
[129] D. J. Comer, D. T. Comer, *IEEE Trans. Circuits Syst.* **2004**, *51*, 8.
[130] C. Cea, G. D. Spyropoulos, P. Jastrzebska-Perfect, J. J. Ferrero, J. N. Gelinas, D. Khodagholy, *Nat. Mater.* **2020**, *19*, 679.
[131] A. Yang, Y. Li, C. Yang, Y. Fu, N. Wang, L. Li, F. Yan, *Adv. Mater.* **2018**, *30*, 1800051.
[132] J. T. Mabeck, G. G. Malliaras, *Anal. Bioanal. Chem.* **2006**, *384*, 343.
[133] M. Berggren, A. Richter-Dahlfors, *Adv. Mater.* **2007**, *19*, 3201.
[134] J. Rivnay, R. M. Owens, G. G. Malliaras, *Chem. Mater.* **2013**, *26*, 679.
[135] D. A. Bernards, G. G. Malliaras, *Adv. Funct. Mater.* **2007**, *17*, 3538.
[136] A. Savva, C. Cendra, A. Giugni, B. Torre, J. Surgailis, D. Ohayon, A. Giovannitti, I. McCulloch, E. Di Fabrizio, A. Salleo, J. Rivnay, S. Inal, *Chem. Mater.* **2019**, *31*, 927.
[137] A. Savva, S. Wustoni, S. Inal, *J. Mater. Chem. C* **2018**, *6*, 12023.

[138] E. M. Thomas, B. C. Popere, H. Fang, M. L. Chabinyc, R. A. Segalman, *Chem. Mater.* **2018**, *30*, 2965.
[139] E. Zeglio, A. L. Rutz, T. E. Winkler, G. G. Malliaras, A. Herland, *Adv. Mater.* **2019**, *31*, 1806712.
[140] E. Stavrinidou, R. Gabrielsson, E. Gomez, X. Crispin, O. Nilsson, D. T. Simon, M. Berggren, *Sci. Adv.* **2015**, *1*, e1501136.
[141] S. Zhao, P. Tseng, J. Grasman, Y. Wang, W. Li, B. Napier, B. Yavuz, Y. Chen, L. Howell, J. Rincon, F. G. Omenetto, D. L. Kaplan, *Adv. Mater.* **2018**, *30*, 1800598.
[142] J. Pas, C. Pitsalidis, D. A. Koutsouras, P. P. Quilichini, F. Santoro, B. Cui, L. Gallais, R. P. O'Connor, G. G. Malliaras, R. M. Owens, *Adv. Biosyst.* **2018**, *2*, 1700164.
[143] E. Bihar, T. Roberts, E. Ismailova, M. Saadaoui, M. Isik, A. Sanchez-Sanchez, D. Mecerreyes, T. Hervé, J. B. D. Graaf, G. G. Malliaras, *Adv. Mater. Technol.* **2017**, *2*, 1600251.
[144] A. Giovannitti, K. J. Thorley, C. B. Nielsen, J. Li, M. J. Donahue, G. G. Malliaras, J. Rivnay, I. McCulloch, *Adv. Funct. Mater.* **2018**, *28*, 1706325.
[145] S.-M. Kim, S. Lee, D. Kim, D.-H. Kang, K. Yang, S.-W. Cho, J. S. Lee, I. S. Choi, K. Kang, M.-H. Yoon, *Nano Res.* **2018**, *11*, 2532.
[146] D. Kim, S.-M. Kim, S. Lee, M.-H. Yoon, *Sci. Rep.* **2017**, *7*, 7716.
[147] D. Kim, S. Park, I. Jo, S.-M. Kim, D. H. Kang, S.-P. Cho, J. B. Park, B. H. Hong, M.-H. Yoon, *Small* **2017**, *13*, 1700331.
[148] S. J. Peter, S. T. Miller, G. Zhu, A. W. Yasko, A. G. Mikos, *J. Biomed. Mater. Res.* **1998**, *41*, 1.
[149] Q. Yang, J. Peng, Q. Guo, J. Huang, L. Zhang, J. Yao, F. Yang, S. Wang, W. Xu, A. Wang, S. Lu, *Biomaterials* **2008**, *29*, 2378.
[150] M. W. Laschke, A. Strohe, C. Scheuer, D. Eglin, S. Verrier, M. Alini, T. Pohlemann, M. D. Menger, *Acta Biomater.* **2009**, *5*, 1991.
[151] S.-K. Kang, R. K. J. Murphy, S.-W. Hwang, S. M. Lee, D. V. Harburg, N. A. Krueger, J. Shin, P. Gamble, H. Cheng, S. Yu, Z. Liu, J. G. McCall, M. Stephen, H. Ying, J. Kim, G. Park, R. C. Webb, C. H. Lee, S. Chung, D. S. Wie, A. D. Gujar, B. Vemulapalli, A. H. Kim, K.-M. Lee, J. Cheng, Y. Huang, S. H. Lee, P. V. Braun, W. Z. Ray, J. A. Rogers, *Nature* **2016**, *530*, 71.
[152] S. P. Lacour, G. Courtine, J. Guck, *Nat. Rev. Mater.* **2016**, *1*, 16063.
[153] R. Chen, A. Canales, P. Anikeeva, *Nat. Rev. Mater.* **2017**, *2*, 16093.
[154] D. Khodagholy, J. N. Gelinas, T. Thesen, W. Doyle, O. Devinsky, G. G. Malliaras, G. Buzsáki, *Nat. Neurosci.* **2015**, *18*, 310.
[155] C. Bodart, N. Rossetti, J. Hagler, P. Chevreau, D. Chhin, F. Soavi, S. B. Schougaard, F. Amzica, F. Cicoira, *ACS Appl. Mater. Interfaces* **2019**, *11*, 17226.
[156] S. Venkatraman, J. Hendricks, Z. A. King, A. J. Sereno, S. Richardson-Burns, D. Martin, J. M. Carmena, *IEEE Trans. Neural Syst. Rehabil. Eng.* **2011**, *19*, 307.
[157] E. Castagnola, L. Maiolo, E. Maggiolini, A. Minotti, M. Marrani, F. Maita, A. Pecora, G. N. Angotzi, A. Ansaldo, M. Boffini, L. Fadiga, G. Fortunato, D. Ricci, *IEEE Trans. Neural Syst. Rehabil. Eng.* **2015**, *23*, 342.
[158] V. Castagnola, E. Descamps, A. Lecestre, L. Dahan, J. Remaud, L. G. Nowak, C. Bergaud, *Biosens. Bioelectron.* **2015**, *67*, 450.
[159] B. P. Tripathi, V. K. Shahi, *J. Phys. Chem. B* **2008**, *112*, 15678.
[160] A. Saxena, B. P. Tripathi, V. K. Shahi, *J. Phys. Chem. B* **2007**, *111*, 12454.
[161] M. Khiterer, D. A. Loy, C. J. Cornelius, C. H. Fujimoto, J. H. Small, T. M. McIntire, K. J. Shea, *Chem. Mater.* **2006**, *18*, 3665.
[162] V. V. Binsu, R. K. Nagarale, V. K. Shahi, *J. Mater. Chem.* **2005**, *15*, 4823.
[163] W. Essafi, G. Gebel, R. Mercier, *Macromolecules* **2004**, *37*, 1431.
[164] S. Park, S. Lee, C.-H. Kim, I. Lee, W.-J. Lee, S. Kim, B.-G. Lee, J.-H. Jang, M.-H. Yoon, *Sci. Rep.* **2015**, *5*, 13088.
[165] K. Melzer, M. Brändlein, B. Popescu, D. Popescu, P. Lugli, G. Scarpa, *Faraday Discuss.* **2014**, *174*, 399.
[166] R. Giridharagopal, L. Q. Flagg, J. S. Harrison, M. E. Ziffer, J. Onorato, C. K. Luscombe, D. S. Ginger, *Nat. Mater.* **2017**, *16*, 737.
[167] C. Cendra, A. Giovannitti, A. Savva, V. Venkatraman, I. McCulloch, A. Salleo, S. Inal, J. Rivnay, *Adv. Funct. Mater.* **2019**, *29*, 1807034.
[168] C. M. Pacheco-Moreno, M. Schreck, A. D. Scaccabarozzi, P. Bourgun, G. Wantz, M. M. Stevens, O. J. Dautel, N. Stingelin, *Adv. Mater.* **2017**, *29*, 1604446.
[169] A. Savva, R. Hallani, C. Cendra, J. Surgailis, T. C. Hidalgo, S. Wustoni, R. Sheelamanthula, X. Chen, M. Kirkus, A. Giovannitti, A. Salleo, I. McCulloch, S. Inal, *Adv. Funct. Mater.* **2020**, *30*, 1907657.
[170] M. Sessolo, D. Khodagholy, J. Rivnay, F. Maddalena, M. Gleyzes, E. Steidl, B. Buisson, G. G. Malliaras, *Adv. Mater.* **2013**, *25*, 2135.
[171] Y. Kim, T. Lim, C.-H. Kim, C. S. Yeo, K. Seo, S.-M. Kim, J. Kim, S. Y. Park, S. Ju, M.-H. Yoon, *NPG Asia Mater.* **2018**, *10*, 1086.
[172] D. Mawad, A. Artzy-Schnirman, J. Tonkin, J. Ramos, S. Inal, M. M. Mahat, N. Darwish, L. Zwi-Dantsis, G. G. Malliaras, J. J. Gooding, A. Lauto, M. M. Stevens, *Chem. Mater.* **2016**, *28*, 6080.
[173] F. N. Ajjan, N. Casado, T. Rębiś, A. Elfwing, N. Solin, D. Mecerreyes, O. Inganäs, *J. Mater. Chem. A* **2016**, *4*, 1838.

Ji Hwan Kim obtained his M.S. in Materials Science and Engineering from Seoul National University of Science and Technology in 2016. He has embarked on his Ph.D. at the School of Materials Science and Engineering, Gwangju Institute of Science and Technology, under the supervision of Prof. Myung-Han Yoon. His current research interests are focused on the structural and compositional modulation of organic mixed conductors for bioelectronic applications.

Seong-Min Kim is currently a postdoc fellow at Georgia Institute of Technology. He obtained his Ph.D. in Materials Science and Engineering with the guidance of Prof. Myung-Han Yoon from Gwangju Institute of Science and Technology. His researches aimed at describing influence of conducting polymer crystallinity on the organic bioelectronic interfaces from both device and biology standpoint. His research interest currently expands on electronic and electrochemical processes in the organic mixed electronic and ionic conductors.

Gunwoo Kim is currently in the master's course of Prof. Myung-Han Yoon group at Gwangju Institute of Science and Technology. In 2019, he received B.S. in School of Materials Science and Engineering at the same institute. He has been researching about fabrication and characterization of polymer-based organic electrochemical transistor active materials.

Myung-Han Yoon obtained Ph.D. in Materials Chemistry with the guidance of Prof. Tobin J Marks at Northwestern University in US. In 2006, he moved to Department of Chemistry and Chemical Biology at Harvard University (Prof. Hongkun Park group) as a postdoctoral fellow and focused on neuronal electronic/fluidic interfaces. He is full professor at the School of Materials Science and Engineering, Gwangju Institute of Science and Technology. His research interest is developing solution-processable functional materials based on conducting polymers, sol–gel metal oxides, and fibrillar hydrogel for printable flexible electronics and bioelectronic interfaces.